# CHAPTER 1

# INTRODUCTION

## 1.1 Background

During the time when Conrad and Marcel Schlumberger come up with the technique of well logging, low resistivity was never on their mind. For them, they hold on a principle that gas- or oil-filled rocks have higher resistivity than water-filled rocks. However, throughout the years, low resistivity pay zone problem has been recognized as a worldwide phenomenon, occurring in basins from the North Sea and Indonesia to West Africa and Alaska.

Within the same reservoir system, when there is a lack of positive contrast in measured electrical resistivity between zones that contain and produce hydrocarbons in commercial quantities and zones that are water-bearing, that is when low resistivity pay occurs. Basically, this problem involved with the evaluation of water saturation, $S_w$. Particularly, the problem appear through the very high values of $S_w$ that can be interpreted from wireline logs of low resistivity strata where a reservoir does not confirm to the assumptions made during the conventional petrophysical evaluation of clean or shaly formations.

In most cases, deep resistivity logs in low resistivity pay read 0.5 to 5 ohm-m. Low contrast is often used in conjunction with low resistivity, indicating a lack of resistivity contrast between sands and adjacent shales. As a result, resistivity values are not necessarily low, but there is little resistivity contrast between oil and water zones. A lot of logging tools lack the vertical resolution to resolve resistivity values for individual thin beds of sand and shale. Instead, the tools provide an average resistivity measurement over the bedded sequence, lower in some zones, higher in others. The problem in identifying low resistivity pay zones using conventional logs has been acknowledges for a long time. It seems that conventional logs cannot determine the petrophysical properties of the low resistivity pay reservoir accurately.

Nuclear Magnetic Resonance (NMR) technology has proved to be essential in modern formation evaluation. Numerous applications of NMR have been introduced over the last few years in different areas of formation evaluation and have added great value to oil and gas production.

NMR is different from those conventional logs. NMR signal amplitudes can provide reservoir properties such as porosity free from lithology effect as well as radioactive sources. In other word, NMR is lithology independent unlike conventional logs. This makes NMR application in low resistivity pay reservoir more reliable than conventional logs. Relaxation times from NMR also give other petrophysical parameters such as permeability, capillary pressure, the distribution of pore size and even hydrocarbon identification.

The usage of NMR in low resistivity pay reservoir has now become worldwide. For example, in East Texas, Oraby and Eubanks *et al.* applied NMR technology to improve determination of pay zones. Kenyon *et al.* on the other hand used NMR technology to estimate pore size distributions in microporous, cherty sandstones. Malaysia also did not miss the chance in applying NMR technology to low resistivity pay reservoirs. This study applied NMR technology in low resistivity pay reservoir in order to help the determination of petrophysical properties.

## 1.2 Problem Statement

In the past few years, a number of new tools like NMR log have been introduced in the oil industry and being used in Malaysian fields generally to enhance the fluid typing, saturation determination as well as permeability forecast. Yet, the application of NMR log in assessing the low-resistivity low-contrast (LRLC) reservoirs in Malaysia has not been fully developed.

Recently, a number of wells drilled by Petronas Carigali Sdn. Bhd. (PCSB) have encountered dry oil and/or gas even though the conventional method interpreted that the percentage of water saturation is up to 70%. This is maybe because of those reservoirs contain high amount of bound water and are actually able to produce clean hydrocarbon. Since there are lack of expertise in Malaysia for NMR analysis, such as in calibration and establishment of the appropriate cut-off standard for transverse relaxation time ($T_2$) fluid relaxation time, a study on using NMR spectral measurements from cores and NMR logs are being commence by Petronas Research Centre Sdn. Bhd. (PRSB).

## 1.3 Research Objectives

This research embarks on the following objectives.

i) Determination of NMR porosity from transverse relaxation time ($T_2$) distribution curve.

ii) To compute the $T_2$ cut-off value and hence distinguishing the clay bound water, capillary bound water and free fluids by evaluating the rock properties using NMR.

## 1.4 Scope of Study

The overall work scope for this research are as follows:

i) Does not involves any experimental work in the lab
ii) Analysis of data that has been received from PRSB
iii) Evaluation of NMR logs on Kumang well which consists of three sample; K3-1-013, K3-1-023, and K3-1-048
iv) Analysing data obtained from laboratory measurement done by CSIRO Lab, Australia to derive the porosity of all samples involved from $T_2$ distribution curve
v) Also, determining $T_2$ cut-off, capillary bound water, free water and also clay bound water.

# CHAPTER 2

# LITERATURE REVIEW

## 2.1 Low-Resistivity Low-Contrast (LRLC) Reservoirs

Low resistivity pay occurs when there is a lack of positive contrast in measured electrical resistivity between zones that contain and produce hydrocarbons in commercial quantities and zones that are water-bearing within the same reservoir. Low contrast indicates a lack of resistivity contrast between sands and adjacent shales. The dilemma with the LRLC zones is that from the interpreted resistivity data, it displays high water saturation, however, oil or even dry oil can be produced.

### 2.1.1 Causes of Low-Resistivity Pay Zones

There are number of causes that can contribute to low-resistivity pay zones. The causes that contribute to low-resistivity phenomenon can generally be divided into two groups. Firstly, is when even though the reservoirs have high actual water saturation, water-free hydrocarbons are being produced. This high water saturation condition is said to have something to do with microporosity (Clavier *et al.* 1984).

The second group is those reservoirs that have higher calculated water saturation compared to the true water saturation. The presence of conductive minerals, for examples; clay minerals, metal sulphides, pyrite and graphite in a clean reservoir rock are said to be responsible for this phenomenon. It is generally known that pyrite is a heavy mineral with good electrical conductivity that is generally as good as or even better compared to the formation water conductivity. The range of resistivity on dry pyrite is from 0.03 to 0.8 Ω m. Since pyrite's conduction is of metallic (electronic) nature, thus, any transmission of current between water and pyrites is based on the conversion from ionic to electronic conduction and contrariwise. This will then leads to polarization at the water-pyrite interfaces, with the corresponding frequency-dependent electrical properties. Therefore, the electrical properties of porous rocks with pyrites are greatly relying on the number and allocation of pyrite as well as the measuring frequency of the electrical current (Clavier *et al.* 1984).

As for low-contrast resistivity pay zones, they can be experienced in those reservoirs with small resistivity difference between water-bearing and oil-bearing zones. For low-contrast resistivity reservoirs, in the water-bearing zone, the resistivity is usually higher than normal since they comprise comparably fresh water. On the contrary, the resistivity in an oil-bearing zone is less than usual and is variable due to the associated water is a mix of fresh and salt water. These oil reservoirs also show a high level of connate water saturation which results in further drop in the formation resistivity (Ayan *et al.* 1987).

### 2.1.2 Conventional Logs in LRLC Reservoirs

Since there are resistivity contrast between the oil zone and water zone, thus, resistivity logs are used to identify the main pay zone. Anyhow, if the pay zone exhibits low resistivity, resistivity logs become incompetent to determine the producing zones and in signifying the water mobility. Due to this constraint, a lot of possibly productive zones with high irreducible water saturation are missed (Hamada *et al.* 2001). In the other hand, it is also hard to recognize the pay zone from resistivity log in the low contrast reservoir due to the aberrant changes in the water and oil zones (Ayan *et al.*1987).

### 2.1.3 Nuclear Magnetic Resonance (NMR) role in LRLC Reservoirs

Commonly, conventional log analysis will recognize the hydrocarbon-bearing zones. However, in low-resistivity reservoirs, it is difficult to figure whether little or no water will be produced, despite the log analyses suggest that the formation has high water saturation. The most promising way in solving this difficulty is by using nuclear magnetic resonance (NMR) log. The NMR log can detect water-free production zones, correlate bound fluid volume and also distinguish hydrocarbon type (Hamada *et al.* 1998 and Zemanek *et al.* 1989). Besides that, it will also shows high contrast NMR relaxation times in those low-contrast reservoirs (Ayan *et al.* 1987).

The strong impact that the rock surface has in contributing to magnetic decay of saturating fluids is what lead to the relationship between NMR measurements and petrophysical parameters. In petrophysical properties assessment, the longitudinal relaxation time ($T_1$) is the parameter of interest, however, NMR only measures the transverse relaxation time ($T_2$), which is influenced by the composition of paramagnetic minerals, for instance (iron-bearing) chlorite, in the low-resistivity pay zones (Hamada *et al.* 2001).

## 2.2 History of Nuclear Magnetic Resonance (NMR)

The first published experiment to measure the effect of Nuclear Magnetic Resonance (NMR) was a failure. In 1936, C. J. Gorter, a Dutch physicist aimed to deliberate the magnetic relaxation processes with the measurement of energy absorption and dispersion in paramagnetic crystals. However, his effort was a disappointment (Waals *et al.* 1996). In spite of that, from his research, Rabi *et al.* (1937) from Columbia University proposed that by studying the magnetism of protons, one can acquire the data on the nuclear cores of atoms. This augury was proven when the first NMR experiments were successfully conducted by two groups of researchers. The first group includes Purcell, Torrey and Pound from Harvard University whom have conducted the NMR experiment in paraffin wax (Purcell *et al.* 1946) while the second group consists of Bloch, Hansen and Packard from Stanford University has done the NMR experiment in liquid water (Bloch *et al.* 1946).

Today, the application of NMR can be seen in many areas such as in chemical industry where NMR provides the fathom of the chemical ambiance at a molecular level. Apart from that, the NMR technology is also being applied in medical disciplines as can be seen in the development of Magnetic Resonance Imaging (MRI) which is an important medical imaging technique nowadays (Appel *et al.* 2004).

Besides in chemical and medical fields, NMR methods were also established in the oil industry. In 1960, using the Earth's magnetic field, Brown *et al.* and Gamson *et al.* have carried out the first NMR measurement in a borehole. However, due to the low intensity of the Earth's magnetic field, the measurement of Earth's field NMR is basically complicated. This causes the Earth's field NMR has not been a big hit in oil industry. On the bright side, the down-hole NMR concept has generated an advanced study which resulted in the growth of fundamental concepts, like the quantification of the movable fluid fraction, interpretation of the measured NMR response in terms of rock permeability and many more (Timur *et al.* 1969). In 1978, Jackson has applied Hahn's finding of the ability to form spin echoes by reversing the direction using radio frequency pulses (Hahn *et al.* 1950) and documented a patent for a pulse echo NMR logging tool. Miller *et al.* (1990) and Kleinberg *et al.* (1992) have proven that this principle is very advantageous and has been the backbone for all designs of modern NMR wireline and LWD tools.

## 2.3 NMR in Oil Industry

NMR works on the nuclei of atoms, by exposing these nuclei to a strong magnetic field. The magnitude of the magnetic field used is dependent on the methods applied. Generally, the Earth's magnetic field strength employed in oil-field applications is lower compared to those used in the chemical applications (Coates *et al.* 1999).

The NMR capability in computing the quantity of matter that adds to the NMR signal has attracted the oil industry towards the NMR phenomenon. The aplenty of the detected NMR signal is directly proportional to the amount of magnetic moments that create this signal. The atoms that make up the rigid rock matrix may consist of NMR-active magnetic moments. However, the response from these nuclei is too fast to be detected by NMR logging tools. Thus, it is postulated that the signal measured by NMR tool comes from pore fluids and also from fluids that are physically and chemically bound to clays. The detected NMR signal can actually be linked to pore volume and in finding formation porosity, provided that if all available pore space is filled with an NMR-active material and the NMR logging parameters are set correctly (Abragam *et al.* 1961).

There are two big challenges in determining the formation porosity using NMR. Firstly, is the acquisition of raw NMR data. For this purpose, the logging tool has to be designed, calibrated and run to detect all magnetic moments of the fluids in the pore space of the investigated region in the formation. Next challenge is in the calculation of porosity from the raw NMR data. Things like type of fluids contributing the NMR signal, necessary signal corrections needed when the chosen log acquisition parameters are given and assigning confidence in the calculated porosity distribution need to be considered by the interpreter (Appel *et al.* 2000).

The correct acquisition of raw NMR data is closely related to the tool design and also tool calibration. In the past few years, service companies have matured in both down-hole and surface equipment used in NMR logging and has improved their calibration methods (Coates *et al.* 1999). Therefore, in these days, the commercial NMR logging service will typically deliver raw NMR data that reflects the investigated formation.

## 2.4 NMR Principles and Basic Theory

The NMR analysis usually consists of two processes. The first one is generating a net magnetization of the reservoir fluids. The magnetic field vector of the magnet polarizes the hydrogen nuclei in the reservoir fluids as the logging tool moves through the borehole which in turn will create a net magnetization along the direction of longitudinal direction ($B_o$). This process can be seen in Figure 2.1. The longitudinal relaxation time ($T_1$) is the time constant that define the exponential build-up of the magnetization.

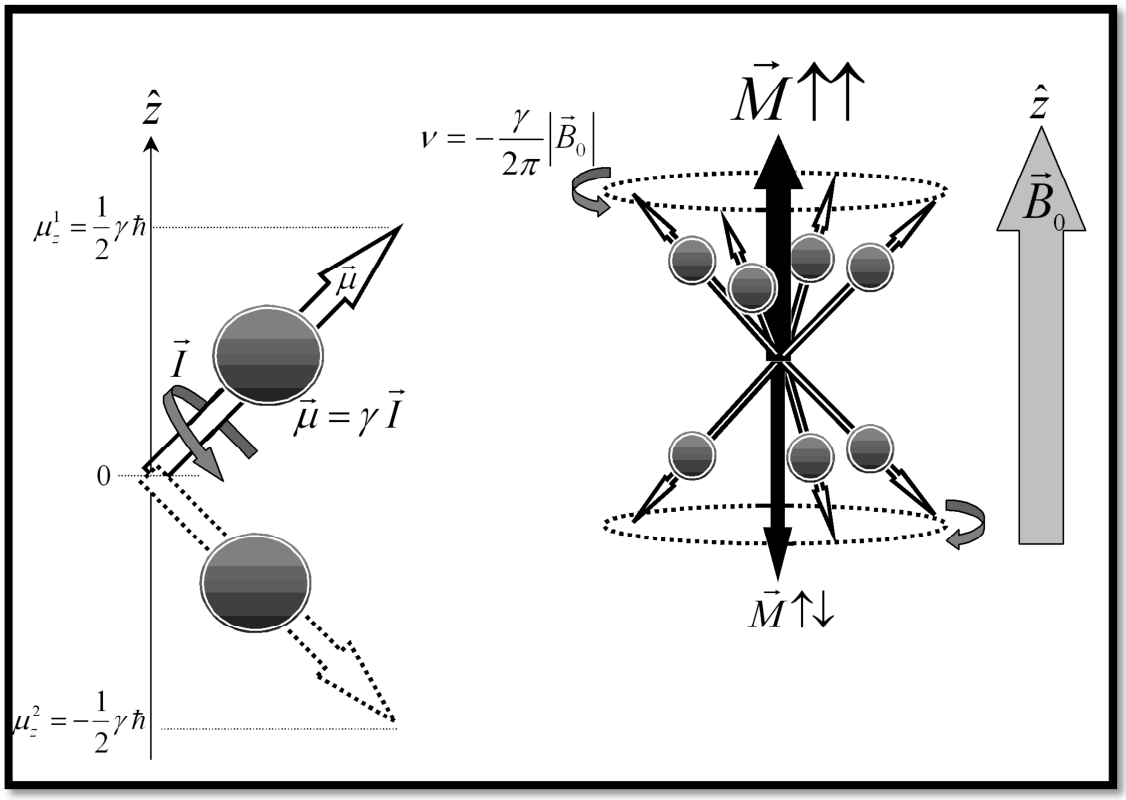


Figure 2.1: Magnetization process (Aguirre *et al.* 2007)

Soon afterward, a train of radio frequency (RF) pulses is assigned to the formation following the polarization time. The first RF pulse rotates the magnetization vector from parallel to $B_o$ into the transverse plane perpendicular to $B_o$ and therefore it is called a 90° pulse. As the magnetization is in the transverse plane, a time-varying signal is produced in the same antenna used to create the pulses by rotating around $B_o$.

Directly after the 90° pulse, an NMR free-induction-decay (FID) signal took place but it decays too fast to be disclosed. The 90° pulse is followed by a series of evenly spaced 180° pulses. These pulses are used to refocus the magnetic moments of the hydrogen nuclei to form coherent spin-echo signal decays which are recorded in between each pair of 180° pulses. The signals are called echoes due to the maximum amplitude they reached is at the midpoint between each pair of 180° pulses and then decay rapidly to zero before the next pulse, which refocuses the magnetic moments produces the next echo. Figure 2.2 shows the NMR measurement process (Aguirre *et al.*2007).

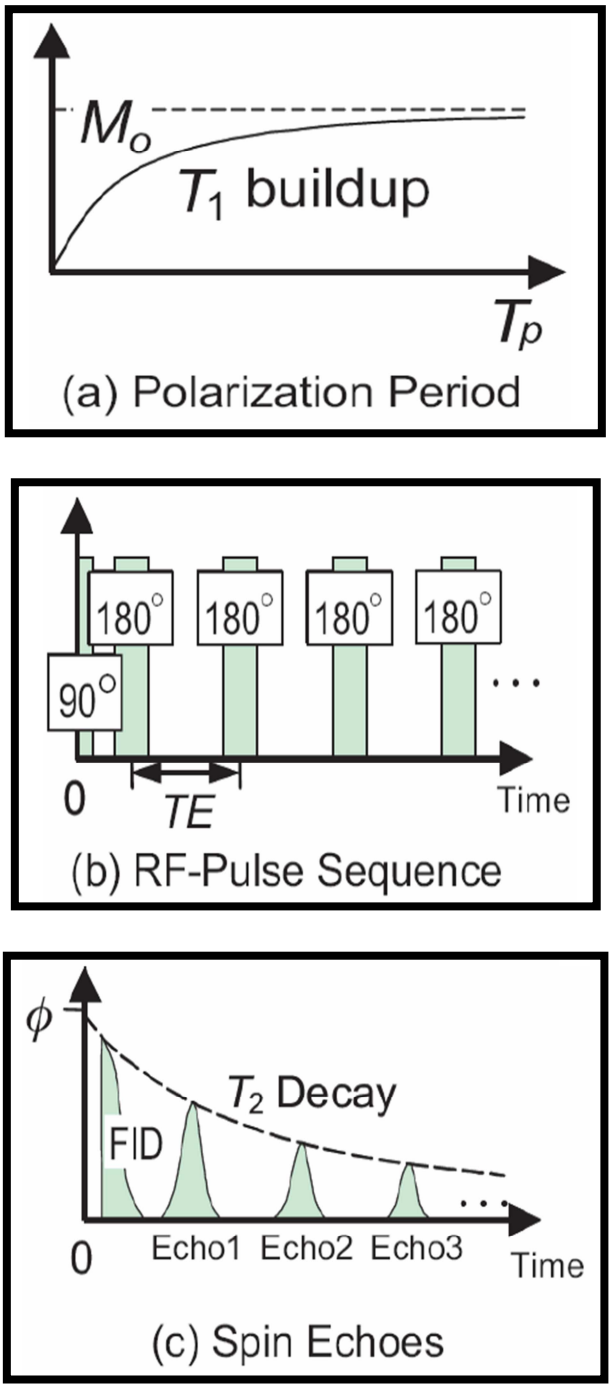


Figure 2.2: The NMR measurement process (Aguirre *et al.* 2007)

The NMR measurements usually provide two major things. First, the echo signal amplitudes depend on the total pore volume. Next, $T_2$ is normally determined by the pore surface-to-volume ratios. Thus, the decay rates or $T_2$ for each component indicates the rate of relaxation which is dominated by relaxation at the grain surface (Aguirre *et al.* 2007).

## 2.5 NMR Log Interpretations

### 2.5.1 $T_2$ Distributions

$T_2$ distributions give a lot of valuable information on reservoir rock and fluid properties and also form the basic outputs displayed on an NMR log. Many other NMR log outputs can be estimated from NMR echo data such as to determine NMR total, bound fluid and free fluid porosities and are also used to compute permeability and reservoir quality estimation. $T_2$ distributions are obtained by fitting spin-echo signals to a sum of approximate 30 single exponential functions, each with amplitude, $A(T_2)$ and associated decay time, $T_2$. The fitting procedure is accomplished using a mathematical technique called inversion. The results from the inversion are the amplitudes, $A(T_2)$ in porosity units corresponding to each $T_2$ value. $T_2$ distribution is defined as a semilog graph of $A(T_2)$ vs $T_2$. NMR total porosity is equals to the area under the $T_2$ distribution. Figure 2.3 shows how a $T_2$ distribution looks like (Freedman *et al.* 2006).

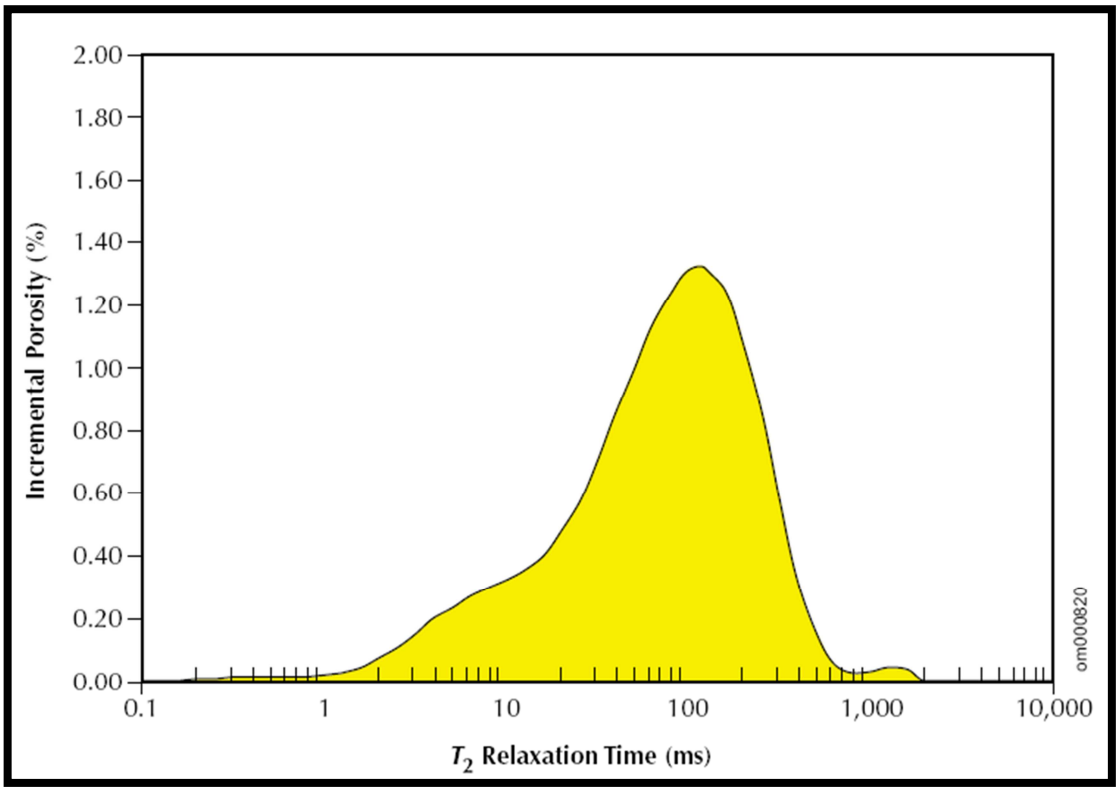


Figure 2.3: $T_2$ distribution (Freedman *et al.* 2006)

In water saturated rocks, $T_2$ distributions are qualitatively related to pore-size distributions. The $T_2$ values ranges from less than 1 ms to several seconds. The reason for the wide range of $T_2$ values in sedimentary rocks is due to the broad distributions of pore sizes. Each $T_2$ in the $T_2$ distribution is proportional to a pore-size diameter. Therefore, those signals from water in small pores are associated with the shorter values of $T_2$ in a $T_2$ distribution and vice versa. Total porosity, bound fluid porosity, free fluid porosity, permeability as well as pore distributions can be estimated by $T_2$ distribution. Scanning-Electron-Microscope (SEM) images of two sandstones that have similar porosities but different measured brine permeabilities by a factor of 37 are shown in Figure 2.4. It can be seen that the $T_2$ distributions show clearly the sandstone of better quality. The lower permeability sandstone has shorter $T_2$ values and more pore-filling clay as indicated by higher bound water volume than the more permeable rock (Freedman *et al.* 2006).

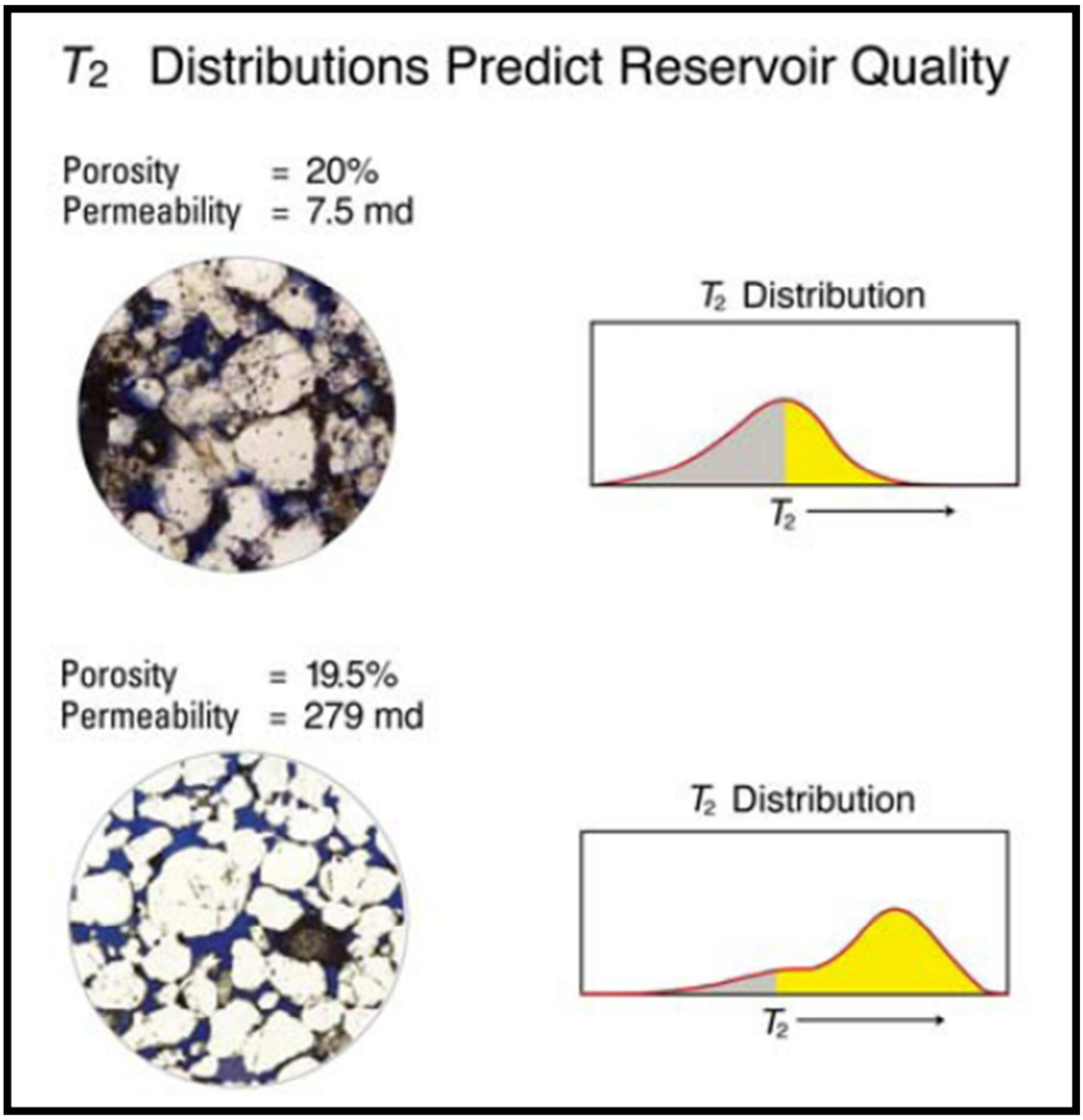


Figure 2.4: SEM images for two sandstones with similar porosities but very different permeability (Freedman *et al.* 2006)

Comparisons between the pore size information contained in $T_2$ distributions with mercury-injection capillary pressure curves are frequently made. It is crucial to note that $T_2$ distributions are related to pore-body sizes while capillary pressure curves provide information on pore-throat sizes. It has been discovered that $T_2$ distributions provide information that complements capillary pressure curves in many sandstones that have pore-body and pore-throat sizes that are well correlated (Freedman *et al.* 2006).

## 2.6 Porosity Concepts

Porosity is the ratio of the volume of voids in a rock to the bulk volume of the rock. It also signifies the most fluid the rock can hold. Total porosity is defined as the ratio of the total volume of pores to the bulk volume of the material despite of the nature of the fluid contained in them while effective porosity is the porosity in which the pores are interconnected by way of a pore-throat and thus, the fluids contained in this volume can be produced. Porosity can be subdivided into primary and secondary porosity. Primary porosity, commonly related to granular, is the porosity developed by the original sedimentation process by which the rock was created. On the other hand, secondary porosity is created by processes which occur after deposition may it be chemical or physical processes. The examples of those processes are dissolution of feldspar grains, dolomitization of carbonates or even fracturing (Hook *et al.* 2003).

### 2.6.1 NMR Porosity

NMR porosity is the determination of actual pore space hydrogen index. Contrary from conventional logs which depend on fluids and surrounding rocks, the basis of NMR porosity is that it relies upon the fluids content of the formation only. This result in much more competent measurements using the NMR compared to conventional logs in providing clay-corrected, non-productive and productive porosities. The intensity of the NMR signal is proportional to the number of hydrogen atoms in NMR tool-dependent rock volume. In zones where there is light hydrocarbon, the hydrogen index will be less than unity. Thus, NMR porosity will normally underestimate true porosity in proportion to the hydrogen index. As for oil and water, NMR results can be signified as the percentage of fluid volume of the rock volume. It is crucial to estimate the pressure and temperature precisely in natural gas reservoirs in order to account for their effect on NMR results since the number of hydrogen atoms in gas reckon strongly on temperature and pressure (Hassoun *et al.* 1997, Hamada *et al.* 1999, Oraby *et al.* 1997, Coates *et al.* 1997).

The standard rock porosity model is shown in Figure 2.5. MSIG refers to the total water content porosity. MPHI represents the total water content porosity (fluid fractions of the rock excluding clay bound fluids). As for MCBW, it is the clay bound water porosity while MFFI denotes the free fluids index which includes all movable fluids (hydrocarbon and free water). MBVI, the capillary-bound water, is defined as all porosities measured with $T_2$ between 3 and 33 ms. Lastly, MBVWT is all bulk volume water (free-, capillary-, and clay-bound water) (Menger *et al.* 1998).

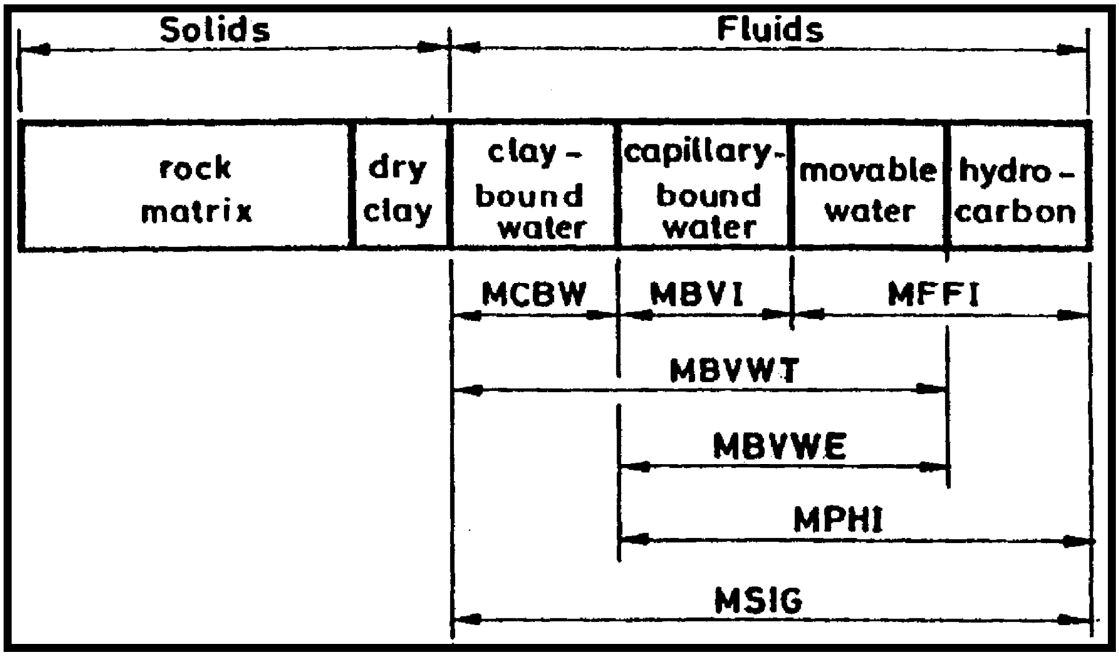


Figure 2.5: The standard rock porosity model for all pore fluids (Menger *et al.* 1998)

NMR porosity can be determined by two methods. The first way is by reading the value of the signal at time zero. The porosity of the rock sample is equivalent to the initial or maximum (at time zero) amplitude of the recorded amplitude sequence from the raw decay curve. The signal at time zero is directly proportional to the number of polarized hydrogen nuclei in the pore fluid.

The amplitude of the spin-echo-train decay can be fit very well by a sum of decaying exponentials, each with a different decay constant. The set of all the decay constants forms the decay spectrum or transverse relaxation time ($T_2$) distribution. Properly defined, the area under the $T_2$ distribution curve is equal to the initial amplitude of the spin echo train. Hence, the $T_2$ distribution can be directly calibrated in terms of porosity (Coates *et al.* 1999).

### 2.6.2 Principle of Porosity Determination by NMR

By comparing the NMR response of the formation with the signal that the same tool obtains when it is exposed to a 100 % porosity environment, net magnetization can be converted into formation porosity. Under certain conditions, the ratio of the net magnetization measured in the formation to the magnetization obtained during calibration in the 100 % porosity environment, will be equal to porosity.

The first condition is the whole pore space is filled with a fluid that contributes to the detected NMR signal. The next condition is the detected NMR signal is not contaminated from fluids in the borehole. Besides that, the delay between subsequent radio-frequency pulses should be sufficiently short to allow enough characterization of the initial signal decay. Apart from that, the logging speed needs to be sufficiently short so that full polarization of all magnetic moments of the pore fluids. The number of magnetic moments per unit volume of the formation fluid also needs to be corrected to the hydrogen index of the calibration fluid. On the other hand, the net magnetization acquired down-hole needs to be corrected to the temperature of the calibration measurement. Finally, for the downhole and calibration measurement, the intensity of the polarizing magnetic field needs to be equal (Appel *et al.* 2004).

## 2.7 Beyond Total Porosity

### 2.7.1 Bound and Free Water

Despite of allowing some logic to be made on the pore size and fluid typing from a thorough evaluation of relaxation decay rates, what is extraordinary regarding NMR is that it also evaluates the volume of the void space by assuming that it is filled with a hydrogenated fluid. This is the capability of NMR to assign the porosity into different components, for example, movable fluids in large pores and bound fluids in small pores. Figure 2.6 shows the partitioning of the $T_2$ distribution of a typical water saturated sandstone into bound (irreducible) and free water by using empirically determined cut-offs (Aguirre *et al.* 2007).

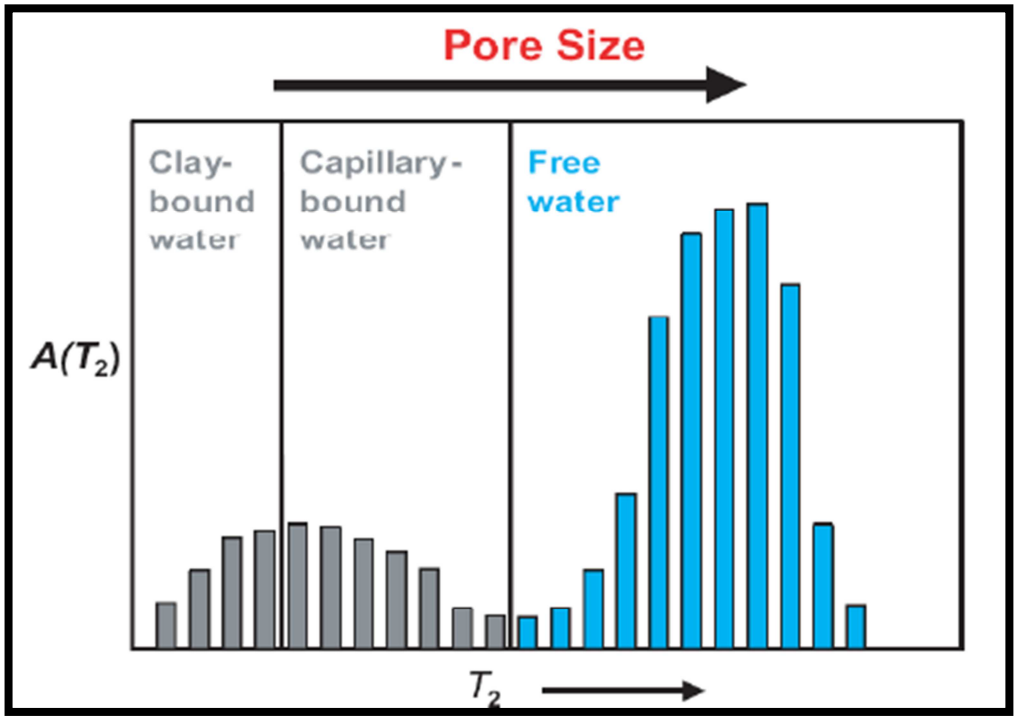


Figure 2.6: Apportion $T_2$ distribution into irreducible and free water (Aguirre *et al.* 2007)

NMR is also able to estimate producible porosity which is called the free fluid index (FFI) which is the amount of water that can be removed from cores by centrifuging them. The estimation of FFI is based on the assumption that the producible fluids reside in large pores, whereas the bound fluids reside in small pores. Bound porosity or bulk volume index (BVI) is the amount of water that cannot be removed from cores by centrifuging them. Since $T_2$ values can be related to pore sizes, a $T_2$ value can be selected below which the corresponding fluids are expected to reside in small pores and above which the corresponding fluids are expected to reside in larger pores. This $T_2$ value is called the $T_2$ cut-off. FFI and BVI can be estimated from a cut-off value of the relaxation time (Coates *et al.* 1999).

Through the partitioning of the $T_2$ distribution, $T_2$ cut-off divides porosity into FFI and BVI as shown in Figure 2.7.

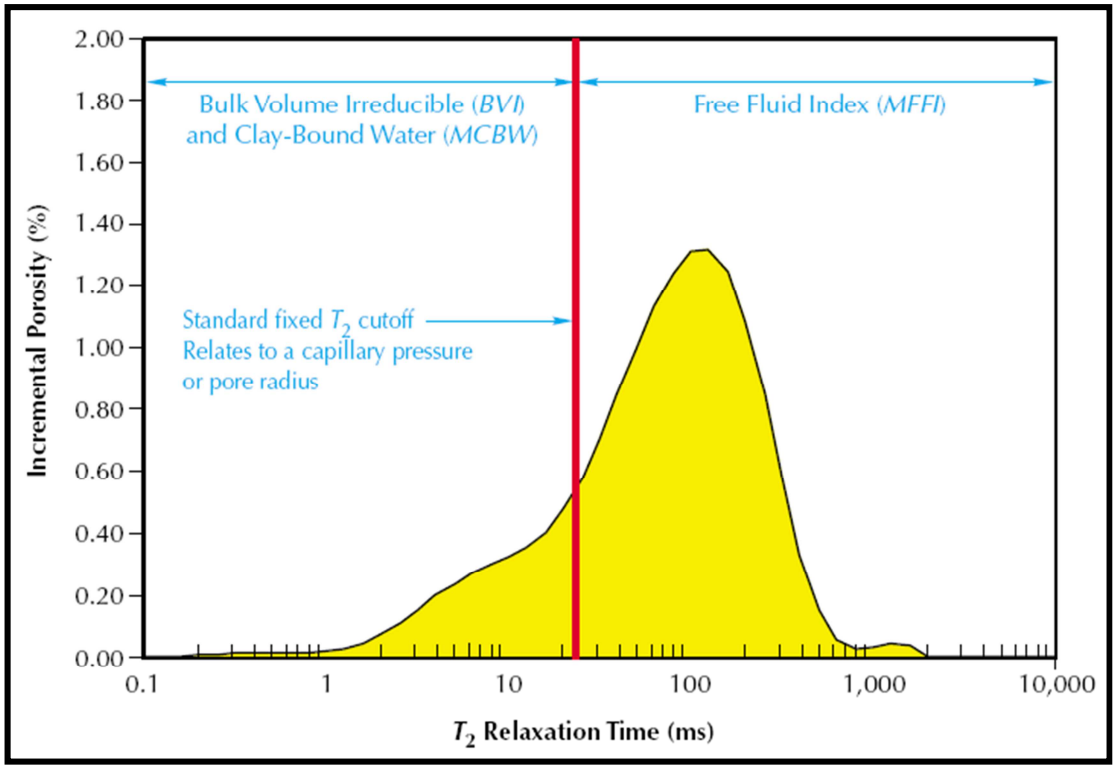


Figure 2.7: Partitioning of $T_2$ Distribution (Coates *et al.* 1999)

Depending on the formations, the cut-off values that divide the relaxation spectra can differ significantly. In 1991, Straley *et al.* has estimated a $T_1$ cut-off for low permeability clay rich sandstones samples taken from formations in western Canada and the US Gulf Coast to be 46 ms. At that moment, since NMR logging was restricted to the measurement of transverse relaxation time ($T_2$), a $T_2$ cut-off was subsequently computed as 30 ms by transforming the measured $T_1$ relaxation response to estimated $T_2$ spectra. For a suite of 86 sandstone samples, a value of 33 ms was confirmed by Straley *et al.* (1994) as the $T_2$ cut-off that yield the best agreement between the free fluid porosity and the volume of fluid that is centrifuged at 100 psi air-brine equivalent capillary pressure. Based from his study, 33 ms is used a default value in quick look NMR log evaluations for sandstone formations. In carbonates formation however, due to the reduced surface relaxivity, the $T_2$ cut-off values are generally higher. Default values of 90 ms have been reported by Coates *et al.* (1999). If representative core material is available, appropriate cut-offs can easily be computed by comparing the measured relaxation spectra before and after the movable fluid fraction has been displaced with an identifiable fluid.

In sandstone formations, the space that enclosed pores can be occupied by different sorts of mineral grains. In a general well-sorted, water-wet sandstones, water which attached to the surface of the sand grains is bound tightly by surface tension. Normally, in these formations, the spaces between sand grains are filled with clay particles. Water also adheres itself to the surfaces of clay particles, and since clays have large surface-to-volume ratios, the relative volume of clay bound water is large. These waters will always remain in the formation and are known as total irreducible water (Aguirre *et al.* 2007).

Water in small pores has larger surface-to-volume ratios with fast relaxation rates and thus short $T_2$ porosity components. This is because, hydrogen nuclei in the thin inter-layers of clay water experienced high NMR relaxation rates due to the water proton that often hit the surfaces since it is close to grain surfaces. Apart from that, the relaxation rates will reflect the surface to volume ratio of the pores if the pore volumes are small enough until the water is able to diffuse easily back and forth across the water-filled pore. This mechanism can be seen in Figure 2.8.

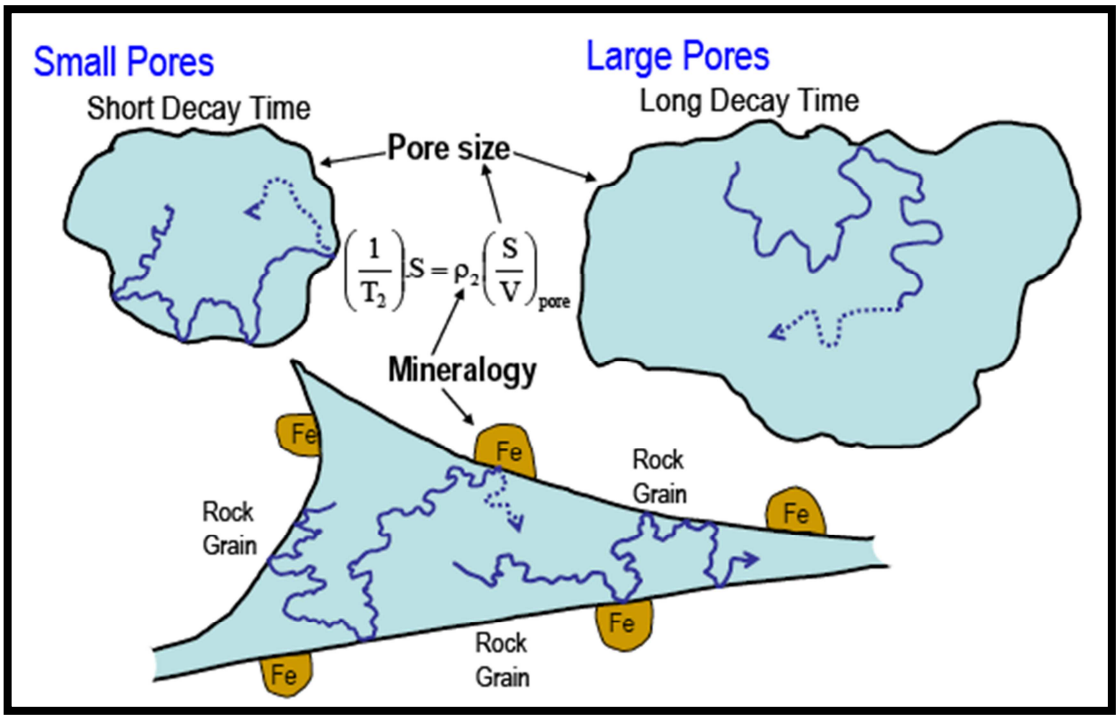


Figure 2.8: Effect of pore size and mineralogy (Aguirre *et al.* 2007)

It takes longer for the hydrogen to diffuse across the pores for large pores with smaller surface-to-volume ratios. This will results in decreasing number of encounters with the surface and leading to lower relaxation rate. This will consequently results in longer $T_2$ component in the NMR measurement. Free water which is found in large pores is not strongly bound to the grain surfaces by surface tension. Therefore, longer $T_2$ time components reflect the volume of free fluid in the formation (Aguirre *et al.* 2007).

### 2.7.2 Clay Identification

Apart from measuring the producible fluid fraction, numerous attempts have been made to apply NMR logging for clay identification. Even under controlled laboratory conditions, only mixed succeed was reported for the unambiguous classification of the NMR response for various clay types (Matteson *et al.* 1998; Chitale *et al.* 2000). In 1994, Straley *et al.* tried to compare the clay bound water volume from membrane potential measurements with the NMR derived fluid volume using a certain cut-off in the $T_2$ distribution. From a set of 45 sandstones, Straley had determined that the deviation between the electrical membrane potential

measurements and the NMR based clay bound water volume is minimized using a $T_2$ cut-off value of 3 ms. Until today, the cut-off value of 3 ms is still being applied in estimating the clay bound water volume from NMR log data.

Figure 2.9 illustrates the approximate ranges of transverse ($T_2$) and longitudinal ($T_1$) relaxation times at which the NMR response of various pore fluids can be expected. It assumes a water-wet formation, and a logging tool possessing a narrow distribution of the gradient of the background magnetic field. The signal originating from gas molecules will not be characterized by a narrow band of distribution times if the pore space is exposed to a wide distribution of the magnetic field gradients. It will instead be spread across the relaxation spectrum according to the distributions widths of magnetic field gradient and gas self diffusivity (Appel *et al.* 2004).

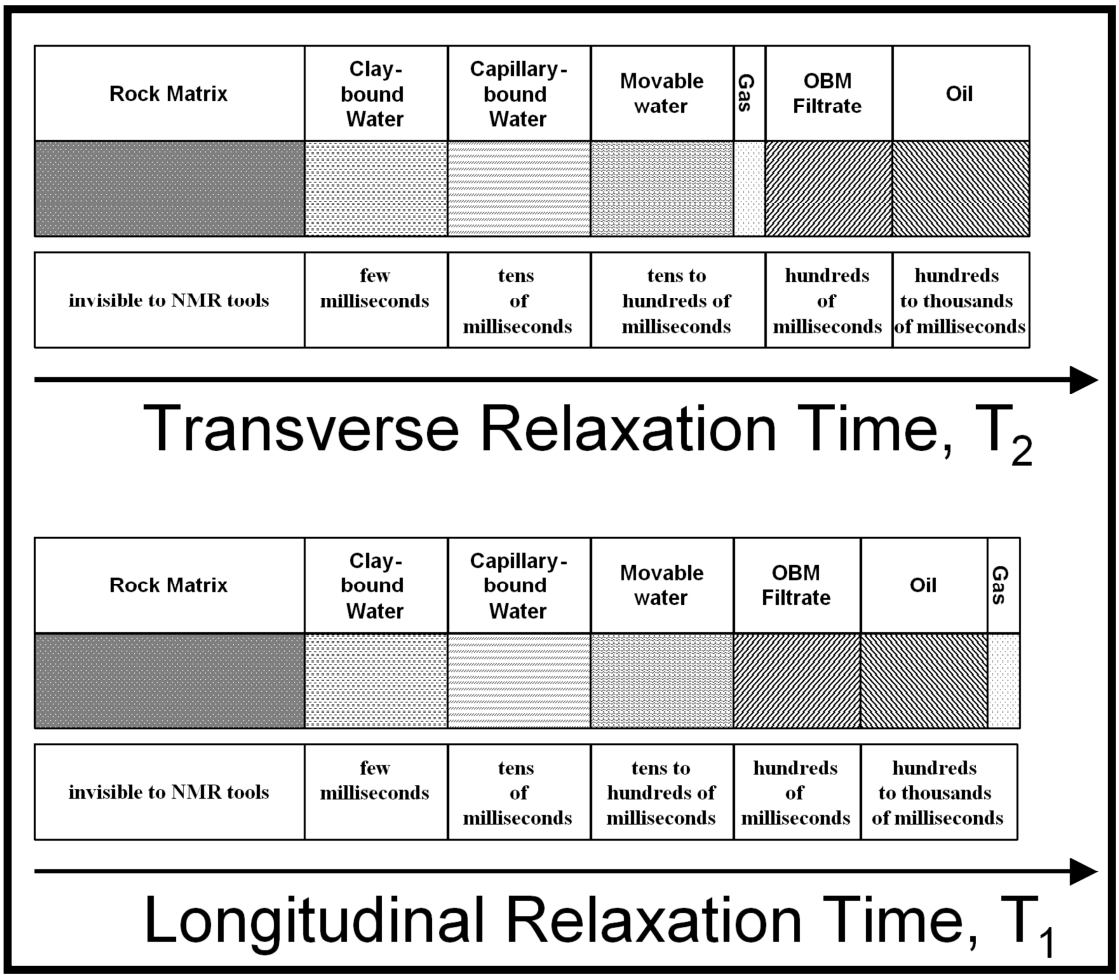


Figure 2.9: Approximate relaxation time response of the various formation fluid components (Appel *et al.* 2004)

## 2.8 NMR and Fluids Type

The new methods which applied the combined effects of $T_1$ and diffusion-based contrast on log response are used for achieving and processing NMR log data allows signals from gas, oil and water to be separated precisely and also measured. The $T_1$ contrast separates water and light hydrocarbons (oil and gas) while the large contrast in the diffusion-induced $T_2$ relaxation times for gas versus liquid helps to separates gas and oil signals. According to the laboratory NMR data, depending on the fluid type, $T_1$ and $T_2$ differ over a couple of degree. In that event, linear gradient field NMR tools have to be dexterous of measuring relaxation times from less than 1 ms to several seconds in order to achieve an accurate fluid typing. The NMR properties for water, oil and gas under typical reservoir conditions is shown in a qualitative way as portrayed by Figure 2.10 (Coates *et al.* 1997 and Menger *et al.* 1998).

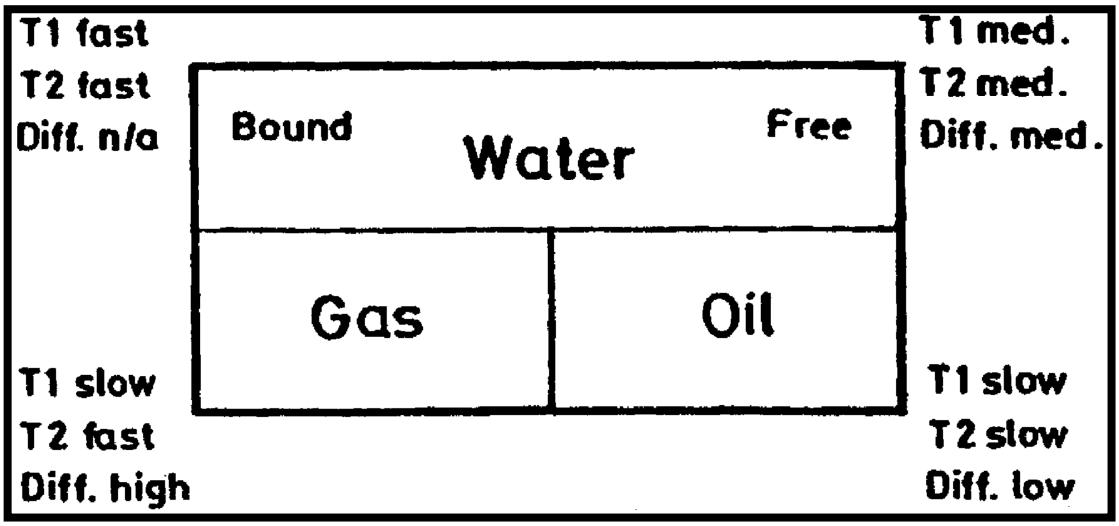


Figure 2.10: NMR parameters under reservoir conditions (Coates *et al.* 1997)

In 1998, Density Magnetic Resonance (DMR) method which combines the total porosity from the NMR tool (TCMR) and the density-derived porosity (DPHI) has been proposed by Freedman *et al.*. This method is use to figure gas-bearing reservoirs by providing gas-corrected total formation porosity and flushed-zone gas saturation. The permeability computed using Coates-Timer equation in gas bearing formation will also be improved with gas-corrected total porosity.

In some low-resistivity reservoirs which contain water saturation even more than 50% are able to produce water-free hydrocarbon due to the clay incorporation. Conventional log analysis can help in ascertain these kinds of reservoirs but it can't figure whether water will be produced or not (Coates *et al.* 1997). Zemanek *et al.* (1989) has came out with a technique to resolve this problem by comparing between irreducible water saturation ($S_{wi}$) derived from laboratory NMR surface area and water saturation ($S_w$) deduced from standard log analysis. Basically, if $S_w$ is less than or equal to $S_{wi}$, water-free hydrocarbon will be produced, and if $S_w$ is greater than $S_{wi}$, water will be produced.

## 2.9 Field Example

### 2.9.1 South Texas

This well is located in the La Salle Delta system and has been identified by showing "[...] strong dip-dominated sandstone trends by Xue and Galloway *et al.* (1985). The logs in Figure 2.11 show data from a portion of the Wilcox formation which, typically consists of separate lithofacies, from sand rich to mudstone shales, potentially deposited in six different depositional systems. From Figure 2.10, in track 1 is the uranium adjusted gamma ray (CGR), calliper (CAL) and the bulk densities from log (RHOB) as well as core analysis (CROB) that uses the inversion of core porosity and matrix density. Track 2 shows density porosity (PDSS), neutron porosity (PNSS) and a neutron density cross plot based porosity (PND) and also core porosity (PCOR). Track 3 compares MRIL total porosity (MSIG) with neutron-density porosity (PND) and core porosity (PCOR).

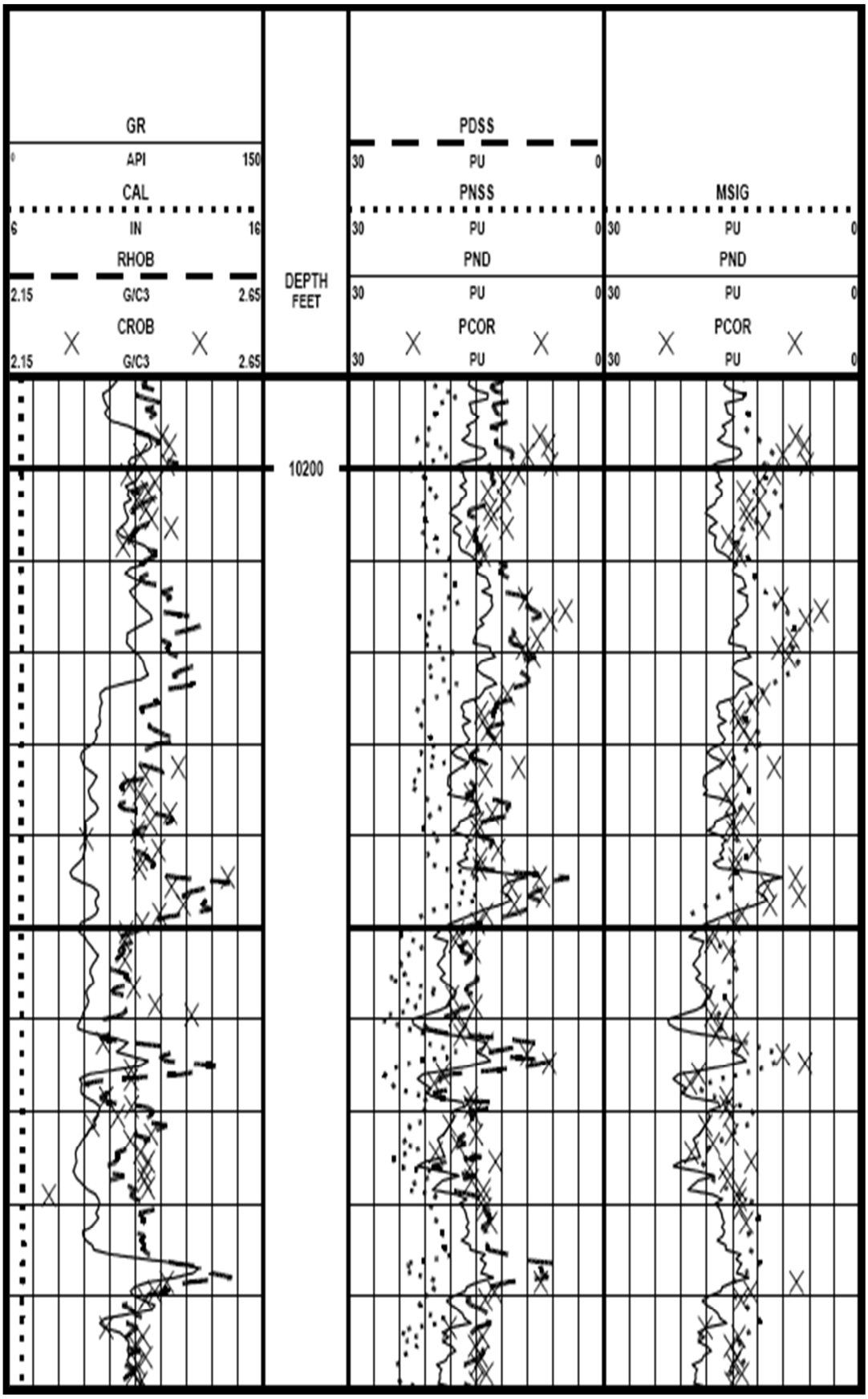


Figure 2.11: Logs and core data over a section of the Wilcox formation from a South Texas (Coates *et al.* 1997)

Generally, the conventionally derived porosity such as PDSS, PNSS and PND exhibit higher values compared to the NMR effective porosity (MPHI) and PCOR. The average difference between PND and MPHI is around 3 – 5 p.u. the high reading of the conventional logs might be caused by significant clay mineral content in the formation, whereas the model to derive porosity from neutron and density logs is based on a clean formation, in this case sandstone formation.

In particular, the neutron porosity is very sensitive to an increase in clay mineral volume as indicated by increased CGR values. This behaviour can be seen clearly at 10286 – 10290 ft. There are also other zones (e.g. 10264 – 10268 ft, 10307 – 10309 ft, 10317 – 10319 ft) where PNSS appears to be influenced by increasing clay mineral content. However, the overestimation of porosity in these intervals is not prominent as the one at 10286 – 10290 ft.

Compared to the conventional logs, MRIL total porosity (MSIG) is in good agreement with PCOR. Anyhow, there are three zones where MSIG and PCOR exhibit different characteristics. In zone 10244 – 10251 ft, core porosity shows decreasing values from about 17 p.u. down to approximately 8 p.u. whereas MSIG slightly increases from 15 to 18 p.u.. In the same interval the conventional logs show the same characteristics as the core data.

The discrepancy between MRIL data and core porosity can be explained by the fact that MRIL's vertical resolution is approximately 3 $ft^2$. The tool "sees" the high porosity formation at 10251 ft correctly, but is not able to resolve the low porosity section (10244 – 10249 ft).

The same applies for depth intervals 10262 – 10277 ft and 10288 – 10290 ft. In all three zones RHOB as well as CROB show an increase in bulk density suggesting that the formation is tighter with less pore volume.

This example clearly demonstrates that conventionally derived porosity can severely suffer from its inherent lithology dependence. Not being affected by such limitations, the lithology independent MRIL total porosity provides more reliable values than the conventional logs (Coates *et al.* 1997).

# CHAPTER 3

# METHODOLOGY

## 3.1 Data Overview

Before proceeding with the methodology, the description of sample from well in study, Kumang-3 which was obtained from Petronas Research Centre Bangi (PRSB) will first be review. Samples of the Kumang-3 well were sent to CSIRO, Australia in April 2008 for the Nuclear Magnetic Resonance spectroscopy (CPMG $T_2$ methods) analysis. The objective is to determine porosity characteristics, clay bound water and to define moveable fluid cut-offs. The samples were all run on a Maran Ultra 2 MHz Spectrometer (Oxford Instruments). Identical inversion parameters (weight parameter of 1.0) were used to obtain the $T_2$ distribution from the signal decay.

The NMR results are of good quality and illustrate the usefulness of NMR to understand the porosity types and fluid mobility in this type of shaly reservoir. There are three samples in study overall from Kumang-3 well namely K3-1-013, K3-1-023 and K3-1-048. Table 3.1 summarizes all three samples in study.

Table 3.1: Kumang-3 Samples Analysed for NMR Spectral Study

| Sample | Depth (m) | Core Porosity (%) | Lithology |
|---|---|---|---|
| K3-1-013 | 1007.65 | 28.3 | Shaly sandstone |
| K3-1-023 | 1010.65 | 29.2 | Shaly sandstone |
| K3-1-048 | 1018.15 | 28.7 | Shaly sandstone |

## 3.2 Data Analysis

As a whole of this study, when the data were obtained from PRSB, data analysis of samples K3-1-013, K3-1-023, and K3-1-048 were done in order to find the porosity and also the $T_2$ cut-off for each sample from the $T_2$ distribution provided. The overall data analysis workflow is summarized in Scheme 3.1.

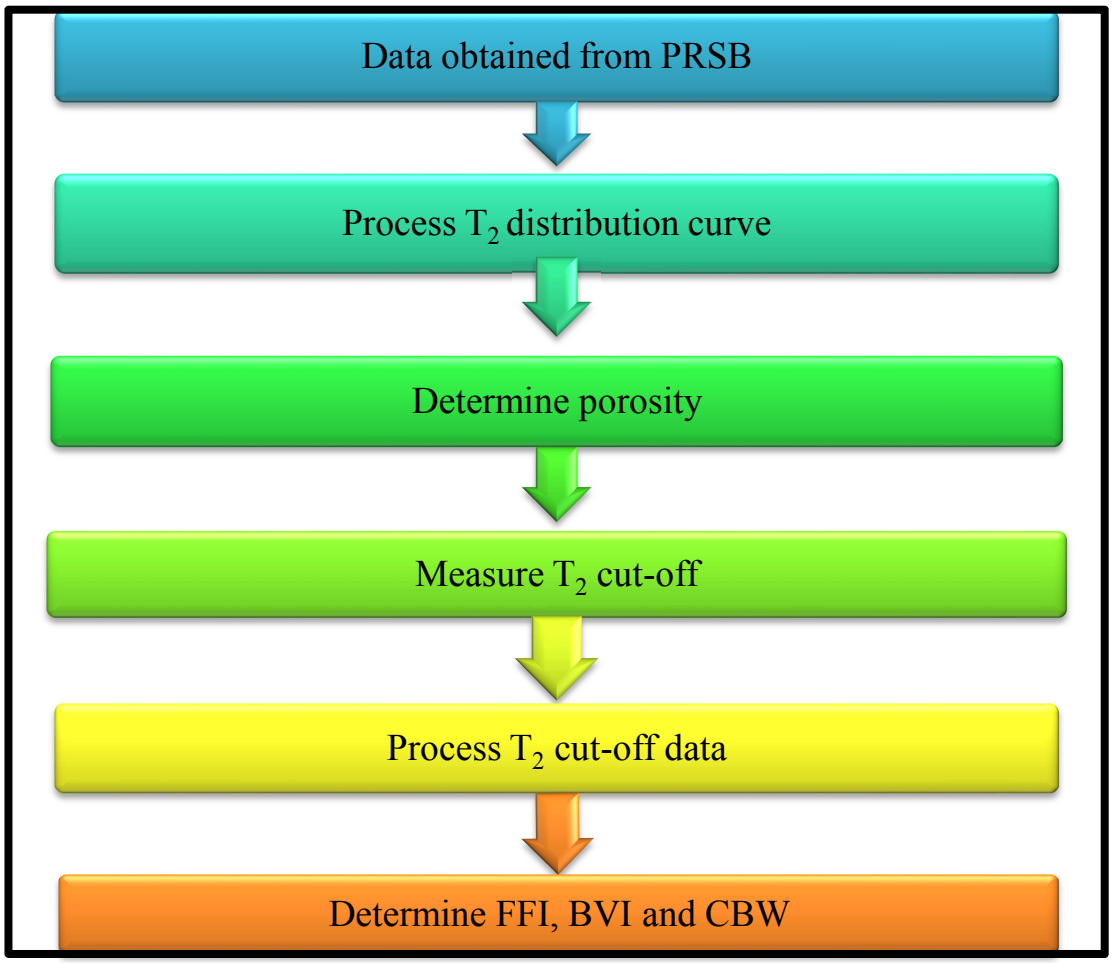


Scheme 3.1: Summary of Data Analysis

### 3.2.1 Determination of Porosity

The method of integrating the area under $T_2$ distribution curve is used to determine the NMR porosity instead of reading the value of the signal at time zero from raw decay curve. This method is chosen because it can provide a more robust result compared to the other method. Besides that, the raw decay curve data are scattered which makes it difficult to find the best fit curve for the decay curve and this can lead to less accurate porosity prediction.

The areas under the $T_2$ distribution curve for all samples are calculated with the help of DPlot software.

### 3.2.2 Determination of $T_2$ Cut-Off

A $T_2$ cut-off can be determined in the laboratory with NMR measurements on core samples. Core samples are analyzed for NMR characteristics at two saturation conditions, $S_w$ = 100 % and (after establishing the appropriate value of saturation from a capillary-pressure curve, or directly desaturating the sample to the appropriate capillary pressure) $S_w$ = irreducible. A centrifuge technique or a porous-plate technique at a specified capillary pressure is used to achieve the latter condition. The $T_2$ distributions are compared as illustrated in Figure 3.1. To determine $T_2$ cut-off, enter the plot from the cumulative porosity axis at the porosity at which the sample is at irreducible condition. Project horizontally to the cumulative porosity curve for $S_w$ = 100 %. Upon intersecting this curve, project down to the $T_2$ axis. The $T_2$ value of the intersection of this projection with the $T_2$ axis is the $T_2$ cut-off.

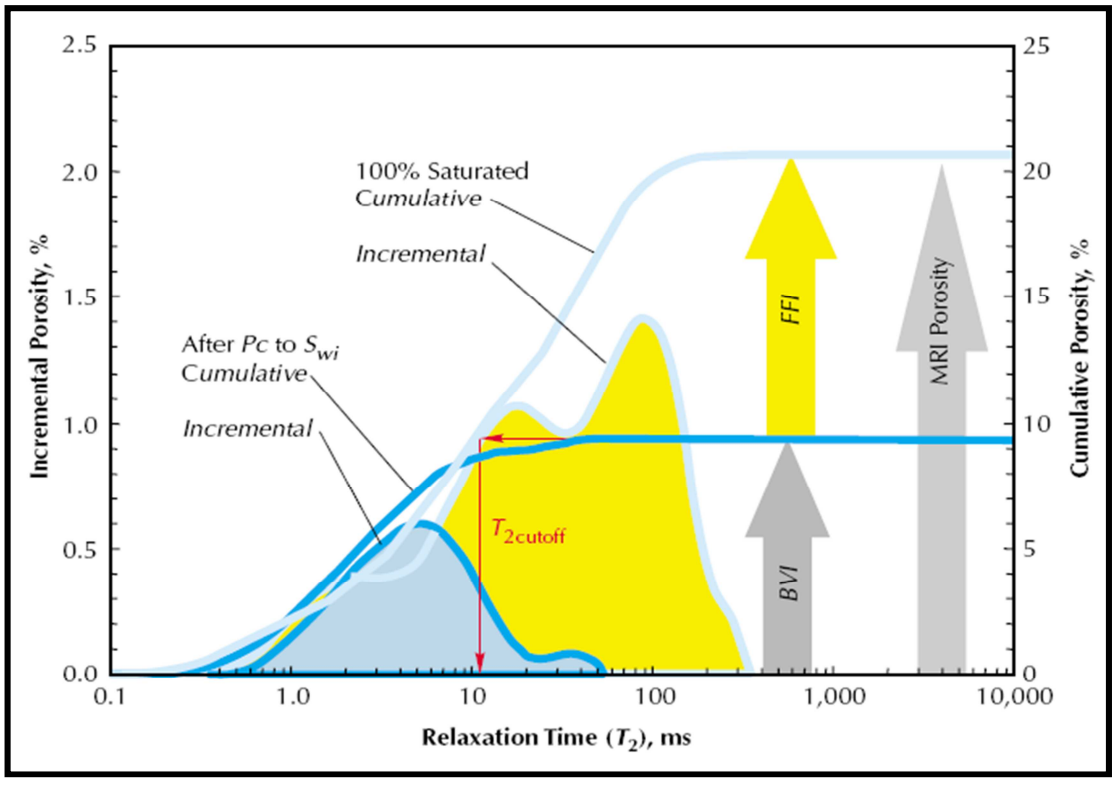


Figure 3.1: NMR measurements on fully saturated and irreducible saturation core samples

# CHAPTER 4

# RESULTS AND DISCUSSIONS

## 4.1 Determination of Porosity

### 4.1.1 Sample *K3-1-013*

The $T_2$ distribution curve of Sample *K3-1-013* is represented in Figure 4.1. The computed area under the curve using DPlot software which also equals to the porosity is 28.0%.

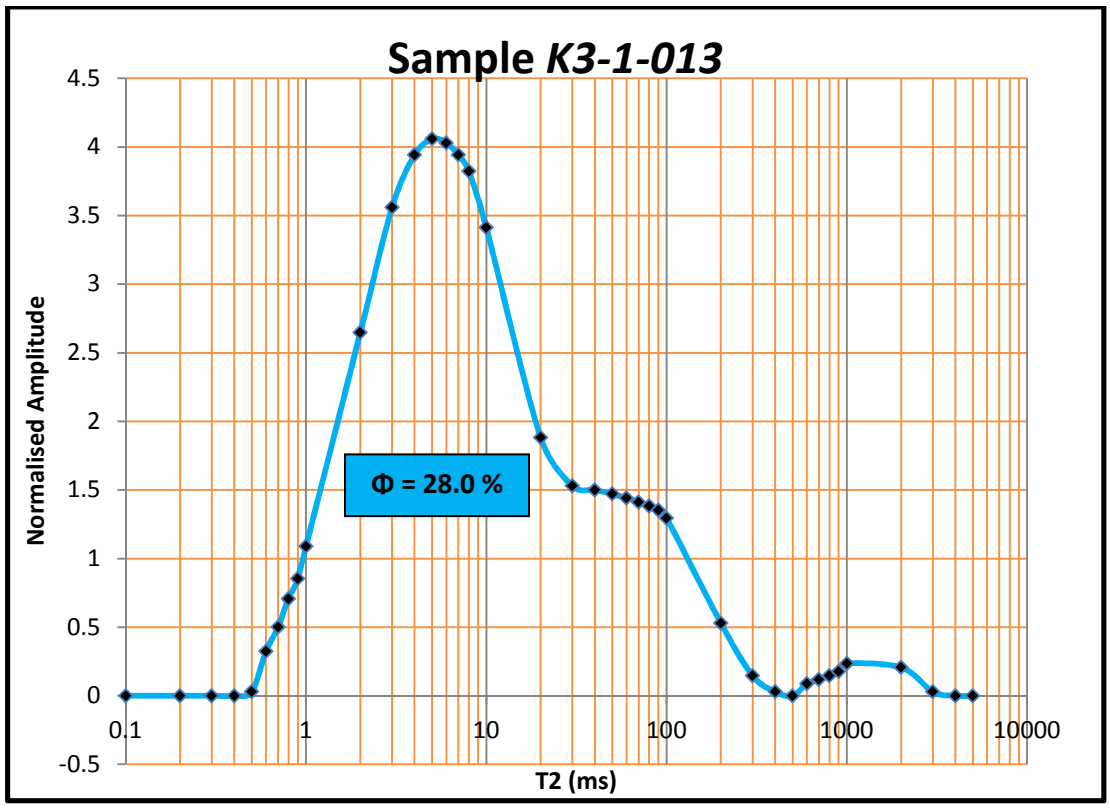


Figure 4.1: $T_2$ Distribution for Sample *K3-1-013*

### 4.1.2 Sample *K3-1-023*

Figure 4.2 shows the $T_2$ distribution curve for Sample *K3-1-023*. The porosity obtained for this sample is 26.5 %.

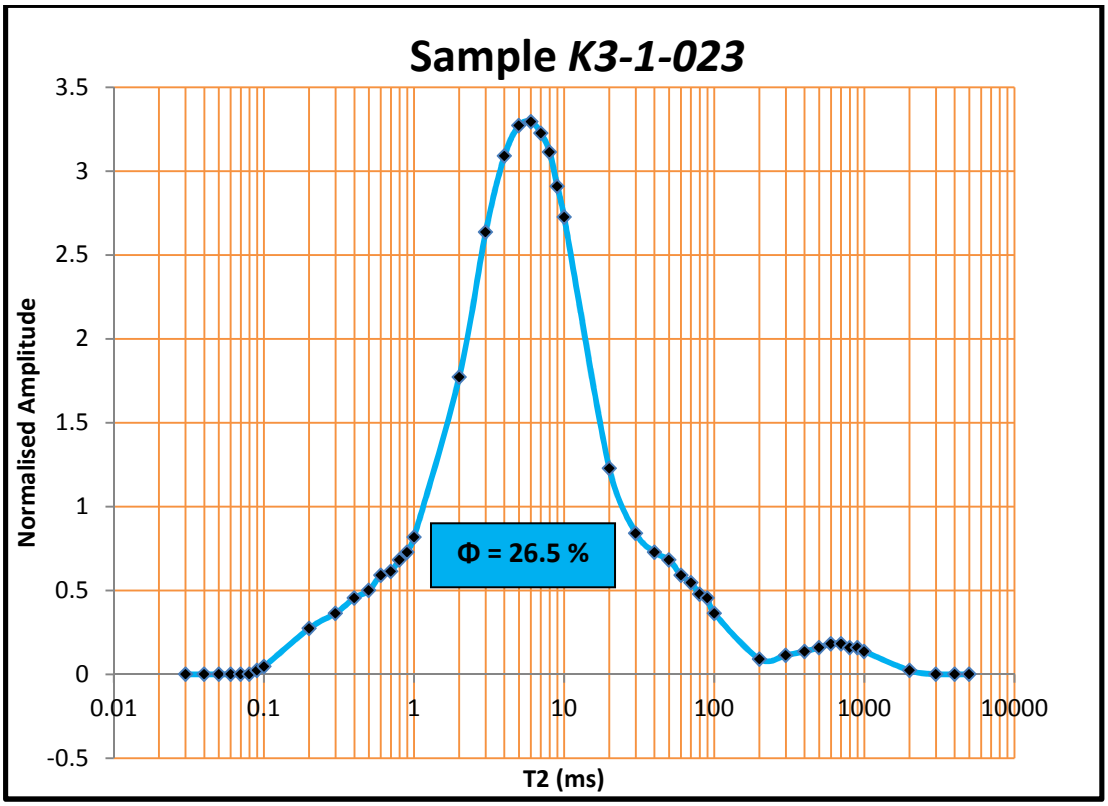


Figure 4.2: $T_2$ Distribution for Sample *K3-1-023*

### 4.1.3 Sample *K3-1-048*

The $T_2$ distribution curve for Sample *K3-1-048* is as shown in Figure 4.3. DPlot software has computed the area under the curve which is also the porosity for this sample to be 25.5 %.

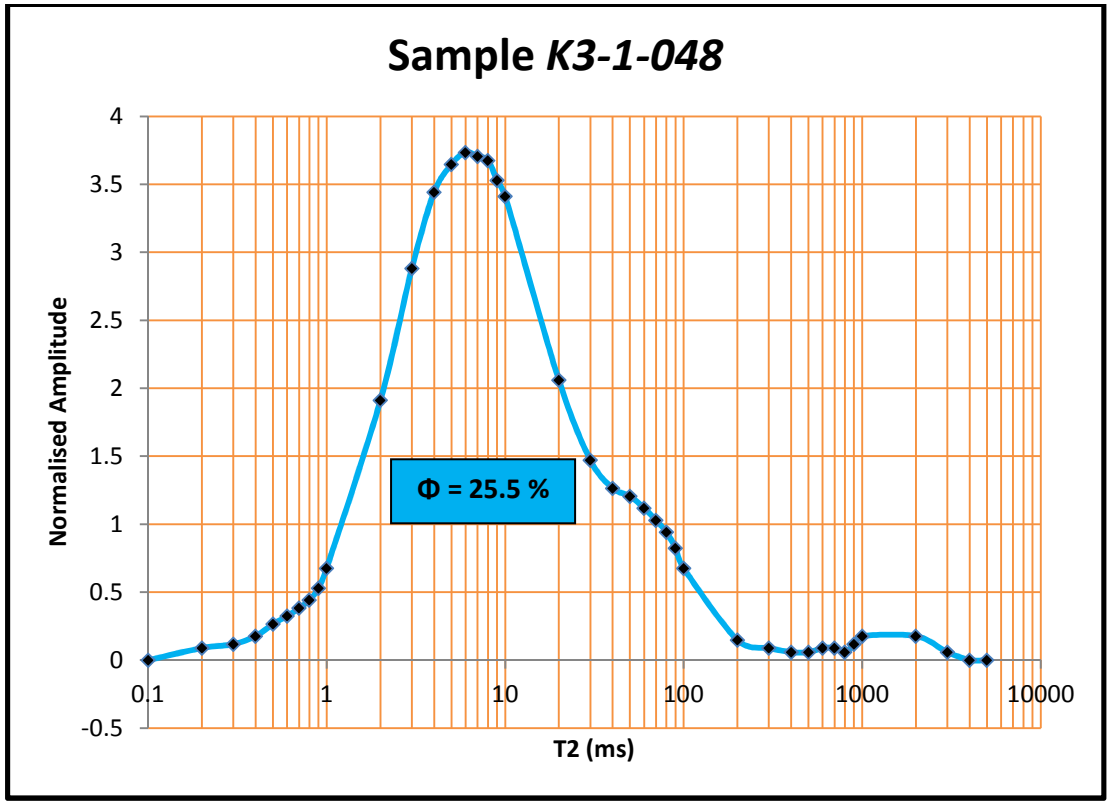


Figure 4.3: $T_2$ Distribution for Sample *K3-1-048*

Table 4.1 summarizes the porosity for all samples and it also includes porosity data obtained by core analysis provided by PRSB so that comparison can be made between both porosities values.

Table 4.1: Summary of Porosities Obtained

| Sample | Core Porosity (%) | NMR Porosity (%) | Differences (%) |
|---|---|---|---|
| **K3-1-013** | 28.2 | 28.0 | 0.2 |
| **K3-1-023** | 29.2 | 26.5 | 2.7 |
| **K3-1-048** | 28.7 | 25.5 | 3.2 |

.

## 4.2 Determination of $T_2$ Cut-off

### 4.2.1 Sample *K3-1-013*

Shown in Figure 4.4 for Sample K3-1-013 are $T_2$ distribution curve (red curve) measured after centrifuging at 100 psi air/brine capillary pressure is superimposed on the respective full saturation $T_2$ distribution curve (blue line). The intersection point between these two curves which also reflect the $T_2$ cut-off is 15 ms.

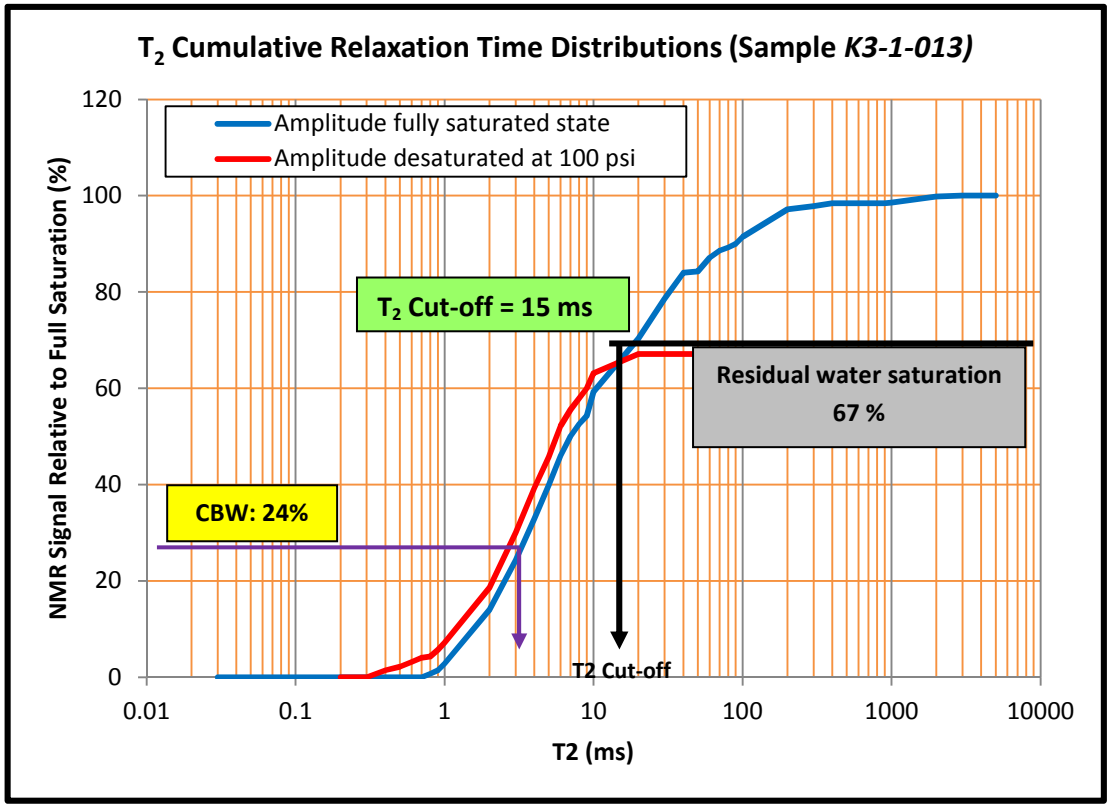


Figure 4.4: Cumulative Curve of NMR Signals (Sample *K3-1-013*)

From Figure 4.6 also, the residual water saturation read 67.2 % while the clay bound water (CBW) amounts to 24 % of total water. Figure 4.5 shows the region of BVI and FFI of this sample from the $T_2$ cut-off value obtained. In this study, the BVI includes all bound water.

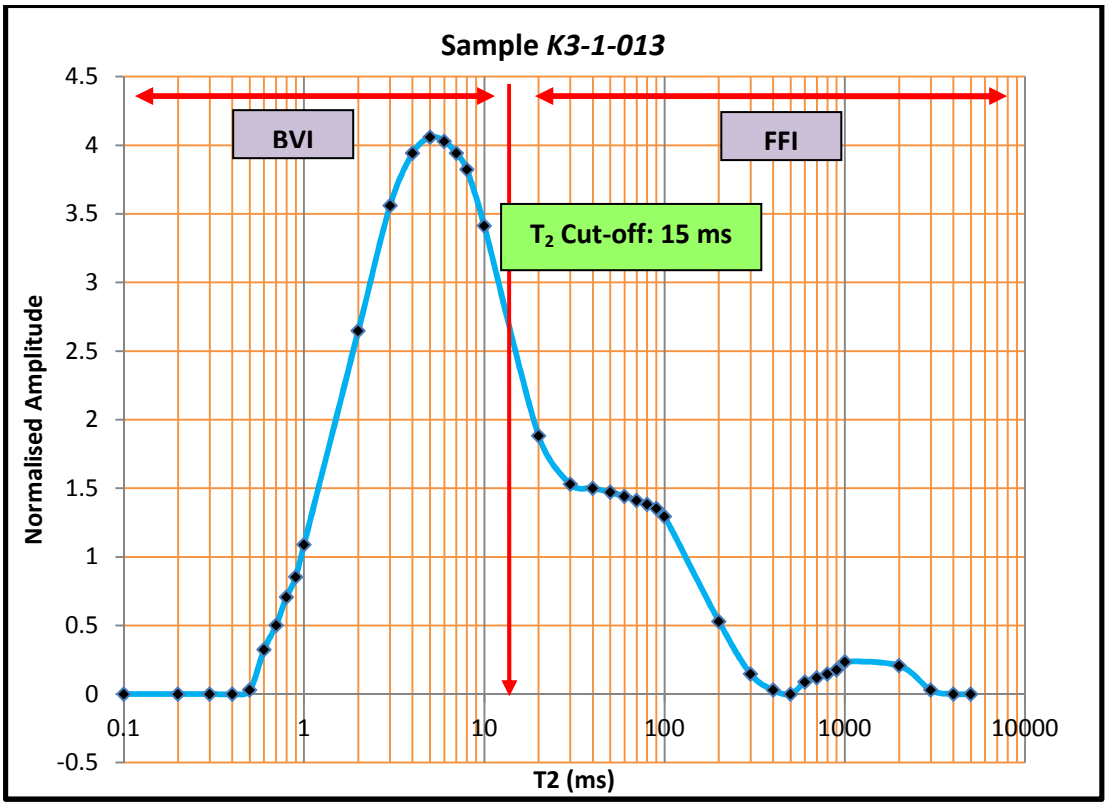


Figure 4.5: Partitioning of $T_2$ Distribution into BVI and FFI (Sample *K3-1-013*)

The curve in Figure 4.5 reflects distributed pore size distribution with a large number of small pores (3 – 20 ms) and a decreasing population of larger pores represented by the shoulder of $T_2$ values around 100 ms.

### 4.2.2 Sample *K3-1-023*

The same method as before is applied to the next sample (Sample K3-1-023). The $T_2$ cut-off is determined from the intersection between the fully saturated and the desaturated at 100 psi curves. The $T_2$ cut-off value obtains for this sample is 16 ms as can be seen in Figure 4.6.

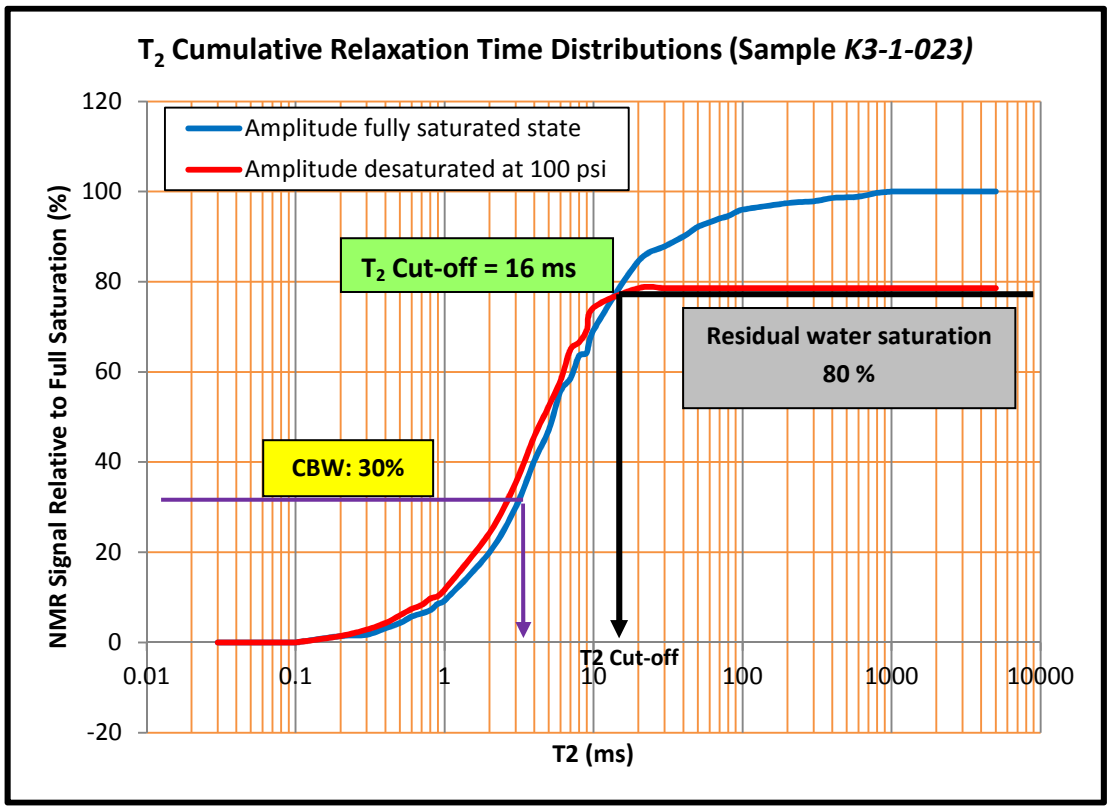


Figure 4.6: Cumulative Curve of NMR Signals (Sample *K3-1-023*)

The water remains after centrifugation is 80% while the CBW which is 30%.

Figure 4.7 shows how the BVI and FFI are being partitioned based on the $T_2$ cut-off value obtained.

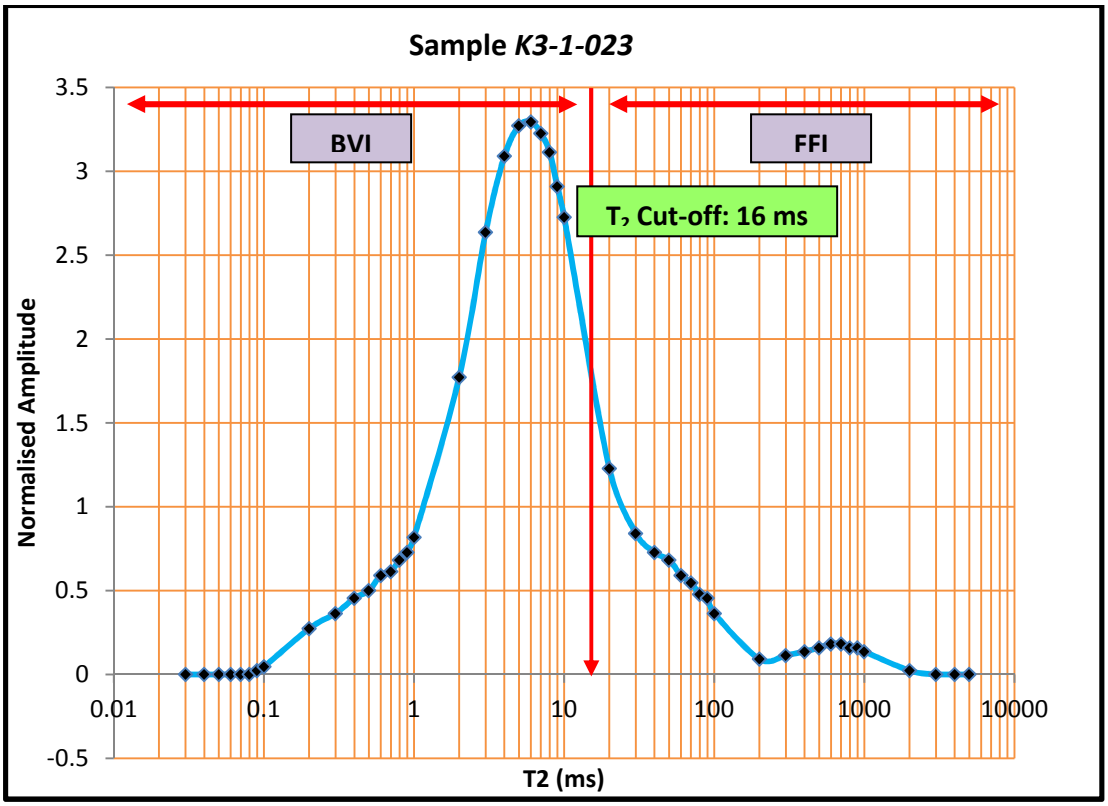


Figure 4.7: Partitioning of $T_2$ Distribution into BVI and FFI (Sample *K3-1-023*)

### 4.2.3 Sample *K3-1-048*

Figure 4.8 shows the method used in determining the $T_2$ cut-off for sample K3-1-048. As can be seen from the curves, the intersection of the curve that desaturated at 100 psi with the fully saturated curve is at 19 ms. This is the value of $T_2$ cut-off for this sample.

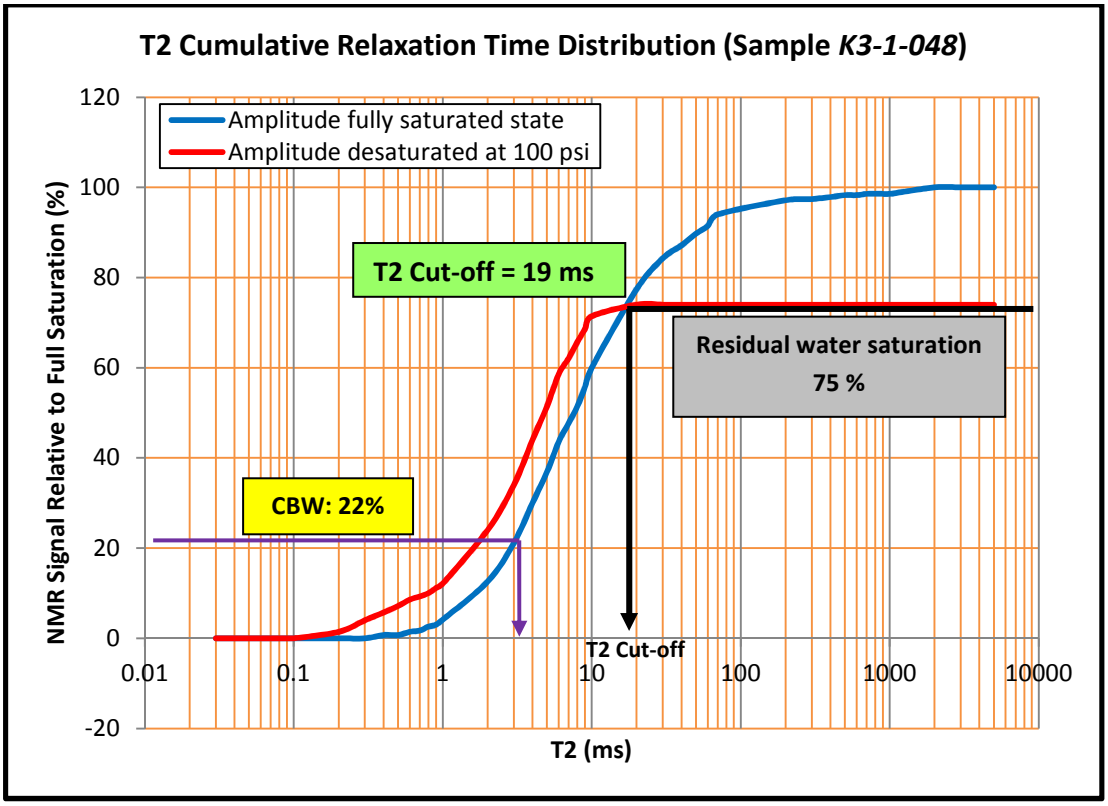


Figure 4.8: Cumulative Curve of NMR Signals (Sample *K3-1-048*)

For this sample, the residual water saturation is around 75 % and the clay bound water is 22 %. How the $T_2$ distribution being divide into BVI and FFI based on the cut-off value of 19 ms can be seen in Figure 4.9.

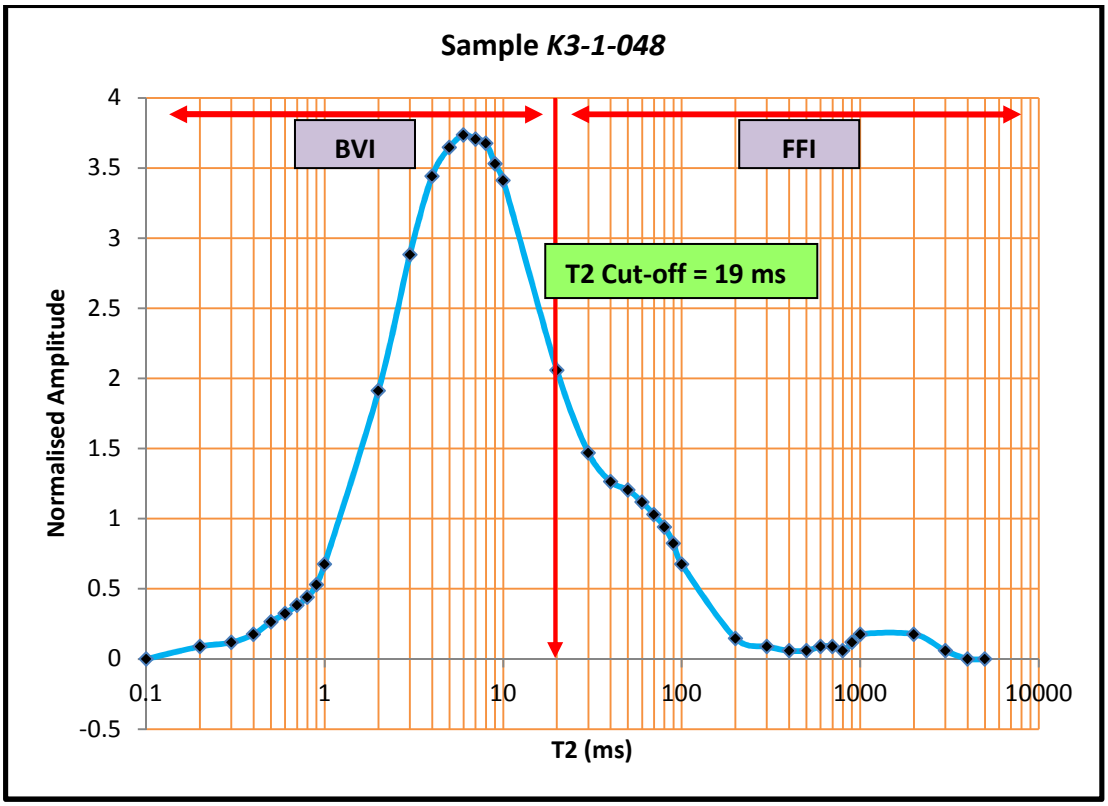


Figure 4.9: Partitioning of $T_2$ Distribution into BVI and FFI (Sample *K3-1-048*)

Table 4.2 summarized the $T_2$ cut-off values, residual water saturation and clay bound water for every samples.

Table 4.2: Summary of $T_2$ Cut-off, Residual Water Saturation and CBW

| Samples | NMR Porosity (%) | $T_2$ Cut-off (ms) | Residual Water Sat. (%) | Clay Bound Water (%) |
|---|---|---|---|---|
| **K3-1-013** | 28.0 | 15 | 67 | 24 |
| **K3-1-023** | 26.5 | 16 | 80 | 30 |
| **K3-1-048** | 25.5 | 19 | 75 | 22 |

## 4.3 Discussion of Results

The porosities from all samples obtained in this study with the help of DPlot software to compute the area under the curve are in the range of 25.5 – 28.0 %. From Table 4.1, it can be seen that the differences between core porosities and NMR porosities is less than 5 p.u.. It can also be seen that all NMR porosities is slightly lower compared to core porosities. This might be because, from the data obtained from PRSB, there are no exact values given for each point on the curve. They only provided the $T_2$ distribution curve. Therefore, in order to digitize the $T_2$ distribution, the value for each point on the curve has been predicted as close as possible. Thus, there might be some predicted points that are not as accurate as the actual values. This might have affected the area under the curve and so does the porosity. However, the core and NMR porosities are still in agreement

For $T_2$ cut-offs, the results obtained from all three samples for Kumang well are quite consistent among them. The values for cut-off are quite systematic, in the range of 15 – 19 ms. However, the obtained $T_2$ cut-offs for all samples are quite low compared to the "default" value of 33 ms for sandstones but it cannot be denied that it is very clearly defined from the intersection. The low cut-off value could reflect a relatively high value of surface relaxivity due to the presence of paramagnetic ions in the rock's constituent minerals (e.g. pore lining clays).

From the desaturated at 100 psi curve, the residual water saturation can be obtained by taking the highest constant value. Residual water saturation represents the amount of water which is left after centrifugation process. From all three samples, it can be seen that the residual saturation values are high, but one would expect that at higher capillary pressure this water could be moved.

The amount of clay bound water in every sample was obtained based on Straley *et al.* studies as mentioned in chapter two of this thesis where the cut-off value of 3 ms is selected to determine the amount of clay bound water.

Compared with downhole data, the NMR data in this study can differ in prevailing temperature and pressure. Overburden pressure will reduce total porosity and in general reduce $T_2$, and stress will especially reduce the number of small, high aspect ratio pores which are more compliant. On the other hand, the fluid viscosity is decreased at high temperature, making $T_2$ slightly larger for a given fluid, so the effects partly cancel.

Besides that, the sample volume in the lab is small, representing only one lithofacies, whereas in the field the NMR sensitive volume is especially laminated shaly sequences will probably average shaly and sandier portions of the formations.

In the lab, the magnetic field is extremely homogenous, so $T_2$ can be measured reliably. In the downhole environment of inside-out NMR, the tool inevitably has a field gradient in the sensitive zone, and this reduces the values of the measured $T_2$ somewhat. Again, this effect can be investigated with more detailed laboratory studies using applied field gradient.

Finally, air-brine capillary pressure need to be adjusted to the prevailing gas-brine or oil brine capillary pressure in the reservoir, depending on pressure, temperature conditions and wettability (if appropriate), before the cut-offs can be applied to a field situation.

# CHAPTER 5

# CONCLUSION

## 5.1 Conclusion

NMR technology is vital in formation evaluation or more specifically in low-resistivity reservoirs. The ability of NMR in differentiating between movable and immovable fluids has helped the log analysts to a more precise estimation. Nevertheless, interpretation using NMR demand discretion as well as experience to guarantee that the appropriate cut-off values are selected based on local laboratory NMR analysis on core samples, and that from the measured and calculated parameters, reliable conclusions can be reached.

NMR has given a big contribution in Kumang well evaluation. First and foremost, it helped in determining the porosity of each sample. Apart from that, NMR also provides quantitative information about pore fluids (clay bound water, capillary bound water, and free water) from the $T_2$ cut-off.

As been mentioned in the results and discussion section, NMR porosity from all three samples were determined from the area under the $T_2$ distribution curve using DPlot software. From the results obtained, it can be seen that the NMR porosity can be correlated with core porosity. From all three samples, the differences between the NMR porosities and core porosities are small which is < 5 p.u difference. The NMR porosity for samples K3-1-013, K3-1-023 and K3-1-048 are 28.0 %, 26.5 % and 25.5 % respectively. NMR porosity can be concluded for being more reliable and robust since the interpretation method used does not involve any matrix or lithology issues. Thus, the uncertainty can be easily avoided with NMR porosity information, which is matrix independent compared if using the conventional logs in determining porosity.

$T_2$ cut-off for all samples was determined by reading the $T_2$ value when the fully saturated state curve intersects the curve which desaturated at 100 psi. $T_2$ cut-off obtained for sample K3-1-013 is 15 ms, K3-1-023 with 16 ms and lastly 19 ms for sample K3-1-048. All the cut-off can be seen obviously from the curve and all values obtained are quite similar to each other.

Residual water saturation for all samples also can be obtained from the curve that desaturated at 100 psi by taking the highest reading of the curve. The residual water saturation for samples K3-1-013, K3-1-023 and K3-1-048 are 67%, 80% and 75% respectively. Clay bound water is determined from the < 3 ms criterion, also from the desaturated curve at 100 psi.

From the $T_2$ cut-off obtained, free fluid index (FFI) and bulk volume irreducible (BVI) can be determined with the value less from the cut-off represents the BVI while the one larger than the cut-off value represents the FFI.

In complex reservoirs, NMR and other log data should be integrated with all other available reservoir information in order to provide the most accurate picture of the reservoir.

## 5.2 Recommendation for Further Studies

Based on this study, analysis on the other properties such as permeability, hydrocarbon typing, oil effects on $T_2$ distribution, gas effects on $T_2$ distribution and others should be done in future studies. Besides that, there are several things that can be put under considerations for further studies:

1. This study only based on the data obtained from PRSB. Therefore, for other coming studies, the students should be given the opportunity to run the NMR machine on his/her own so that it would be easier for the students to understand all the data obtained from the NMR analysis.

2. If the analysis to be done only depends on the data obtained from any company, then, sufficient data should be provided from the company since insufficient data will make it difficult for the analysis to be done.

3. Understanding the concept of NMR analysis is really crucial in order to determine the properties of interest.

# APPENDICES

## Laboratory Procedure (received from CSIRO)

### NMR Analysis

The analyses were performed at the CSIRO ARRC Petrophysical Laboratory facility using a Maran Ultra spectrometer operating at a fixed frequency of 1.920 MHz (Nominally 2 MHz). The spectrometer operates at a fixed temperature of 35 °C and has a very uniform field strength, so that no externally generated field gradients are present.

Calibration for signal amplitude vs water content was obtained using standard samples of water doped with nickel chloride to reduce the relaxation time to values similar to pore water in rocks. Standards were run before, during and after the series of samples. The average value of the standard calibration factor for several runs of 15 mL, 10 mL, and 5 mL water samples was used in the analyses. Water acquisitions were made with full polarization (2 seconds is enough for 321 microsecond $T_1$ of the nickel doped water), and with 256 scans. The standard normalization for water content was made for the response of 1 mL of water with 256 scans at the fixed receiver gain of 64. All NMR based water contents use this calibration.

### Brine Sample

10 mL of brine was measured with a pipette and into a vial. Samples were analysed with an echo spacing suitable for the brine, 500 μs. A full length Carr-Purcell-Meiboom-Gill (CPMG) echo train was acquired, with 256 scans. The signal was fit to a single dominant $T_2$ component and also inverted to give a narrow $T_2$ distribution. $T_1$ was obtained using the inversion-recovery procedure.

**Water Saturated Sample $T_2$ Analysis**

Each saturated sample, wrapped in waterproof film, was analysed using a CPMG pulse sequence with an inter-echo spacing of 240 μs ($\tau$ = 120), 8192 or 12000 echoes to obtain the transverse relaxation ($T_2$) decay curve. 256 or 512 scans were used for water saturated samples. This guarantees full polarization. Signal to noise ratio was computed with the "GETSNR" command at the end of each run, and the run repeated with more scans if signal-to-noise ratio (SNR) was less than 100.

A computerized least-squares fitting routine with regularization (WINDXP) was used to obtain the multiple exponential decay time distribution from the data, giving a $T_2$ distribution for each sample divided into 128 logarithmically-spaced bins (30 μs – 5 s). The regularization parameter was fixed at 1, gives a distribution of relaxation times, or $T_2$ spectrum which is somewhat smoothed, and comparable with the data that would be obtained by downhole tools running slowly with full polarization and the shortest possible echo spacing.

NMR total porosity is determined from the amplitude of the initial NMR signal prior to the spin decay. This total amplitude is obtained by two methods: 1) The actual, recorded initial value of the NMR signal which is first recorded at t = 253 μs after the 90° pulse, called "initial amplitude method"; and 2) From the sum of the $T_2$ bins after inversion, called the "sum $T_2$ method".

**Desaturated Samples $T_2$ Analyses**

Each desaturated sample, wrapped in film, was analysed using an identical CPMG pulse sequence with an inter-echo spacing of 240 μs, 4096 echoes to obtain the transverse relaxation ($T_2$) decay curve. 512 scans were used to obtain good signal to noise characteristics > 100. A 3 s relaxation delay (wait time) was used, otherwise acquisition was similar to the water-saturated case. The inversion procedure to obtain the $T_2$ spectrum was identical.

## REFERENCES


[1] Oraby, M. and Eubanks, D., "Determination of Irreducible Water Saturation using Magnetic Resonance Imaging Logs (MRIL): A Case Study from East Texas," *SPE 37772*, March 1997.

[2] Kenyon, W., Howard, J., Sezginer, A., Straley, C. and Matteson, A, "Pore Size Distribution and NMR in Microporous Cherty Sandstone," *SPWLA*, June 1989.

[3] Clavier, C., Coates, G. and Dumanoir, J., "The Theoretical and Experimental Basis for the Dual Water Model for the Interpretation of Shaly Sand," *The Log Analyst,* 1984.

[4] Ayan, C., Haq, S. A. and Boyd, A., "Integration of NMR Wireline Tester, Core and Open Hole Log Data for Dynamic Reservoir Properties," *SPE 53273*, March 1987.

[5] Hamada, G. M., Al-Blehed, M. S., Al-Awad, M. N. and Al-Saddique, M. A., "Petrophysical Evaluation of Low-Resistivity Sandstone Reservoirs with Nuclear Magnetic Resonance Log," *Journal of Petroleum Science and Engineering,* 2001.

[6] Hamada, G. M. and Al-Awad, M. N. J., "Petrophysical Evaluation of Low Resistivity Sandstone Reservoirs," *SCA 9851*, September 1998.

[7] Zemanek, J., "Low Resistivity Hydrocarbon Bearing Sand Reservoir." *Journal of Petroleum Technology and Formation Evaluation,* 1989.

[8] Van der Waals, J. H., "Encyclopedia of Nuclear Magnetic Resonance" (p. 677 – 681). *John Wiley and Sons,* 1996.

[9] Rabi, I. I., "Space Quantization in a Gyrating Magnetic Field," *Physical Review,* 1937.

[10] Purcell, E. M., Torrey, H. C. and Pound, R. V., "Resonance Absorption by Nuclear Magnetic Moments in a Solid," *Physical Review,* 1946.

[11] Bloch, F., Hansen, W. W. and Packard, M., "The Nuclear Induction Experiment." *Physical Review,* 1946.

[12] Appel, M., "Nuclear Magnetic Resonance and Formation Porosity," *Log Analysts*, 2004.

[13] Brown, R. J. S. and Gamson, B. W., "Nuclear Magnetism Logging," *SPE-1305-G*, 1960.

[14] Timur, A., "Producible Porosity and Permeability of Sandstones Investigated through Nuclear Magnetic Resonance Principles." *The Log Analyst*, 1969.

[15] Hahn, E. L. “Spin Echoes,” *Physical Review*, 1950.

[16] Miller, M. N., Paltiel, Z., Gillen, M. E., Granot, J. and Bouton, J. C., “Spin Echo Magnetic Resonance Logging: Porosity and Free Fluid Index Dtermination,” *SPE 20561*, 1990.

[17] Kleinberg, R. L., Sezginer, A., Griffin, D. D. and Fikuhara, M., “Novel NMR Apparatus for Investigating an External Sample,” *Journal of Magnetic Resonance,* 1992.

[18] Coates, G. R., Xiao, L. Z. and Prammer, M. G., “NMR Logging, Principles and Applications,” *Halliburton Energy Services,* 1999.

[19] Abragam, A., “The Principles of Nuclear Magnetism,” *Oxford University Press,* 1961.

[20] Appel, M., Freeman, J. J., Perkins, R. B. and Dijk V. N. P., “Reservoir Fluid Study by Nuclear Magnetic Resonance,” *Annual Logging Symposium Transactions,* 2000.

[21] Aguirre, O., Glorioso, J. C., Repsol, Y. P. F., Morales, J. And Mengual, J. F., “Porosity with Nuclear Magnetic Resonance in Naturally Fractured Clastics Reservoirs in the Devonian of the Bolivian Sub-Andean,” *SPE 107192,* April 2007.

[22] Freedman, R., “Advances in NMR Logging,” *SPE 89177,* 2006.

[23] Hook, J. R., “An Introduction to Porosity,” *Well Log Analysis*, 2003.

[24] Hassoun, T. H. and Zainalabedin, K., “Hydrocarbon Detection in Low Contrast Resistivity Pay Zones, Capillary Pressure and ROS Determination with NMR Logging in Saudi Arabia,” *SPE 37770,* March 1997.

[25] Hamada, G. M., Al-Blehed, M. S. and Al-Awad, M. N., “NMR Logs Find Reservoirs By-Passed by Conventional Analysis,” *Journal of Oil and Gas*, 1999.

[26] Oraby, M., Chafai, N., Hussing, R. B., Massengill, D. R., Clark, J. S. and Pletcher, D., “A New NMR Interpretation Technique Using Error Minimization with Variable $T_2$ Cut-off,” *SPE 38734,* October 1997.

[27] Coates, G. R., Menger, S. and Miller, D., “Applying Total and Effective NMR Porosity to Formation Evaluation,” *SPE 38736,* 1997.

[28] Menger, S. and Prammer, M., “Can NMR Porosity Replace Conventional Porosity in Formation Evaluation,” *SPWLA,* May 1998.

[29] Straley, C., Morriss, C. E., Kenon, W. E. and Howard, J. J., "NMR in Partially Saturated Rocks – Laboratory Insights on Free Fluid Index and Comparison with Borehole Logs," *Well Log Analysts,* 1991.

[30] Straley, C., Rossini, D., Vinegar, H., Tutunjian, P. And Morriss, C., "Core Analysis by Low Field NMR," *SCA 9404*, 1994.

[31] Matteson, A., Tomanic, J. P., Herron, M. M., Allen, D. F. And Kenyon, W. E., "NMR Relaxation of Clay-Brine Mixtures," *SPE 49008*, 1998.

[32] Chitale, D. V., Garner, J. and Sigal, R., "Significance of NMR $T_2$ Distributions from Hydrated Montmorillonites," *Log Analysts,* 2000.

[33] Coates, G. R., "A New Characterization of Bulk Volume Irreducible using Magnetic Resonance," *SPWLA,* 1997.

[34] Xue, L. Nad Galloway, W. E., "High-Resolution Depositional Framework of the Paleocene Middle Wilcox Strata, Texas Coastal Plain," *AAPG Bulletin,* 1985.

**BIODATA OF STUDENT**


Name: *Lydia bt. Mohd Yusof*

Date of Birth: *2nd July 1988*

Place of Birth: *Taiping, Perak*

Programme: *MSc Petroleum Engineering*

Supervisor: *A.P. Dr. Zuhar Zahir b. Tuan Harith*

Co-Supervisor: *Mr. Elias Abllah*